chemosensors

MDPI

Review

Micro-Magnetofluidic System for Rare Cell Analysis: From Principle to Translation

Kangfu Chen [1] and Zongjie Wang [2,3,*]

[1] Department of Pharmaceutical Sciences, Leslie Dan Faculty of Pharmacy, University of Toronto, Toronto, ON M5S 3M2, Canada; kangfu.chen@utoronto.ca
[2] Department of Biomedical Engineering, McCormick School of Engineering, Northwestern University, Evanston, IL 60208, USA
[3] Chan Zuckerberg Biohub Chicago, Chan Zuckerberg Initiative, LLC, Chicago, IL 60607, USA
* Correspondence: zongjie.wang@northwestern.edu

Abstract: Rare cells play essential roles in the initiation and progression of diseases and therefore their analysis is of great interest. The micro-magnetofluidic system is one of the emerging platforms that have been proposed for the rapid, sensitive, and cost-effective analysis of rare cells. Given its unprecedented throughput, micro-magnetofluidic systems have attracted substantial research interest in the last decade—multiple designs have been proposed, validated, and even advanced to the stage of clinical trials. This mini review aims to provide a timely summary of the relevant progress in the field thus far. We reviewed the concepts and realizations of micro-magnetofluidic devices based on the interaction between nanoparticles and on-chip micro-magnets. Their real-world applications in rare cell analysis were also highlighted and explained. In addition, we discussed the major challenges in the development and translation of micro-magnetofluidic into the clinic, including multi-marker capability and large-scale manufacturability.

Keywords: microfluidics; magnetic nanoparticles; rare cell analysis; cell sorting

Citation: Chen, K.; Wang, Z. Micro-Magnetofluidic System for Rare Cell Analysis: From Principle to Translation. *Chemosensors* **2023**, *11*, 335. https://doi.org/10.3390/chemosensors11060335

Academic Editors: Pedro Salazar, Soledad Carinelli and Takahiro Arakawa

Received: 26 April 2023
Revised: 22 May 2023
Accepted: 30 May 2023
Published: 6 June 2023

1. Introduction

There are approximately 37 trillion cells present in the adult human body [1]. Among this gigantic number of cells, some cell populations, although relatively rare, play critical roles in the initiation and progression of diseases and the success of tissue regeneration. Given the critical role of rare cells, their quantitation and isolation have become an intriguing research topic.

So far, the efforts can be roughly divided into two categories: optimization of existing approaches and development of new techniques. The existing approaches include the use of off-the-shelf equipment, such as flow cytometry [2–9]. Indeed, multiple protocols have been developed to use various flow cytometers to robustly detect rare cell populations down to 0.001% [4]. However, these approaches require recording a very large number of events (e.g., 1×10^9) [4] due to the inherent noise level of flow cytometers [3]. This scale of events is not practical for real-world analysis, even with the most advanced high-speed flow cytometer (~60,000 events/s) [10,11]. Therefore, the majority of the research efforts have been paid to develop new techniques, mainly microfluidics [12–16], for the isolation and analysis of rare cells.

Microfluidics is the "science and technology of systems that process or manipulate small amounts of fluidics using channels with dimensions of tens to hundreds of micrometers" [12]. The feature size of microfluidic devices is inherently at the same scale of mammalian cells (~10–20 μm in diameter). As a result, microfluidics can offer very precise manipulation of mammalian cells with a single-cell resolution [17] and this has led to the assembly of highly complicated cell-laden microwells [18], droplets [19], or microtissues [20] for physiology [21] and drug screening [22]. The use of microfluidics

for CTC isolation began in 2007 [23] and it opened a completely new field. Thus far, over 50 different types of microfluidic devices have been designed and validated for the analysis of rare cells, such as circulating tumor cells [24–26]. Undoubtedly, microfluidics has become one of the mainstream technologies in the analysis of rare cells.

To distinguish rare cells from their excessive counterparts, researchers often took advantage of a combination of nucleic acids and/or proteins specific to the rare cells [27]. In realization, these specific 'biomarkers' are often detected through antibodies that generate fluorescence [28], Raman spectroscopy [29,30], mass spectrometry [31,32], or magnetic signals [33]. Among these readouts, magnetic signals confer the best throughput of isolation due to their non-serial, highly parallelized working principle [34]. In fact, the most advanced micro-magnetofluidics have achieved a throughput of 3.2 billion cells per hour [35], which outperforms the throughput of fluorescence-activated cell sorting, Raman spectroscopy, and mass spectrometry by order of magnitude. Taking advantage of high throughput, the magnetic sorting of rare cells from patient whole-blood samples can be completed in 1–2 h, enabling routine analysis of CTCs in large-scale clinical studies [36].

The term "micro-magnetofluidics" was proposed in recent years to describe the combination of magnetophoresis and microfluidics [37,38]. It has several advantages, including (1) an easy trigger mechanism that can be created with a permanent magnet [39]; (2) precise control of cell movement in the microchannel [40]; (3) continuous- and high throughput flow separation of cells [41]; and (4) easy integration with other techniques such as optical and acoustic manipulation [42]. Thus far, two realizations of micro-magnetofluidic approaches for rare cell analysis have been proposed—magnetic deflection and magnetic ranking.

Here, we review the concepts and realizations of magnetic deflection and magnetic ranking for rare cell quantitation. Their real-world applications are also highlighted and explained in a case-by-case manner. We hope this review provides a timely summary of the state-of-the-art technologies being developed so far and help to shape the future development of novel devices to overcome the current limitations in magnetic-based cell isolation and analysis.

2. Rare Cells: Definition and Examples

A cell is considered 'rare' when the number of cells of that subpopulation represents less than 0.01% of the total cell populations in a tissue or biofluid [43,44]. These cells, although occur as a minimal population, may play critical roles in disease progression and tissue regeneration. Below are a few examples highlighting the essentiality of rare cells in important bioprocesses.

For disease progression, one vivid instance is the initiation of cancer metastasis [45], where the primary tumor evolves and generates delayed secondary tumors in distal organs [46]. While many theories have been proposed to explain the process of cancer metastasis, the most accepted mechanism is through the formation of circulating tumor cells (CTCs) [47,48] (Figure 1A). In brief, CTCs are rare cells that emigrate from the primary tumor, enter and circulate within the peripheral blood, and eventually settle down in different organs for growing [49]. CTCs are generally considered as the seed of metastasis given their critical role during cancer migration [50,51] and therefore have attracted significant attention as a general biomarker for monitoring and predicting cancer progression [52–54]. However, one critical challenge of using CTCs is their rarity—the number of CTCs is extremely low, usually at the scale of a few CTCs in millions of normal cells [55–57].

For tissue regeneration, a representative example is the use of human hematopoietic stem/progenitor cells (HSPCs) for transplantation. HSPCs only represent 0.2% to 0.5% of the leukocyte population (or 0.0003–0.0008% of the blood cell population) in peripheral blood [58], but have the full potency to produce all types of blood cells (e.g., lymphocytes and monocytes, Figure 1B). Therefore, the transplantation of HSPCs has been essential to the immune reconstruction post the treatment of leukemia [59–61]. Besides, rare cells may modulate the fate of a specific regenerative therapy given to a patient. It has been reported that rare undifferentiated stem cells in therapeutic cells, such as cardiomyocytes [62] and

beta cells [63], may undergo uncontrolled growth in vivo in animal models [64,65] and eventually convert regenerative therapies into stem cell cancers [66–69].

Thus far, over 50 different types of microfluidic devices have been designed and validated for the analysis of rare cells, including circulating tumor cells [70,71], circulating tumor clusters [72–74], circulating cancer stem cells [75–77], circulating fetal cells [78,79], and circulating endothelial cells [80] in peripheral blood, as well as contaminating tumor cells [81] in therapeutic cell products. Multiple strategies have been proposed, such as filtration, inertial fluidics, deterministic lateral displacement (DLD), and immunomagnetic sorting [13]. In this article, our focus is immunomagnetic sorting.

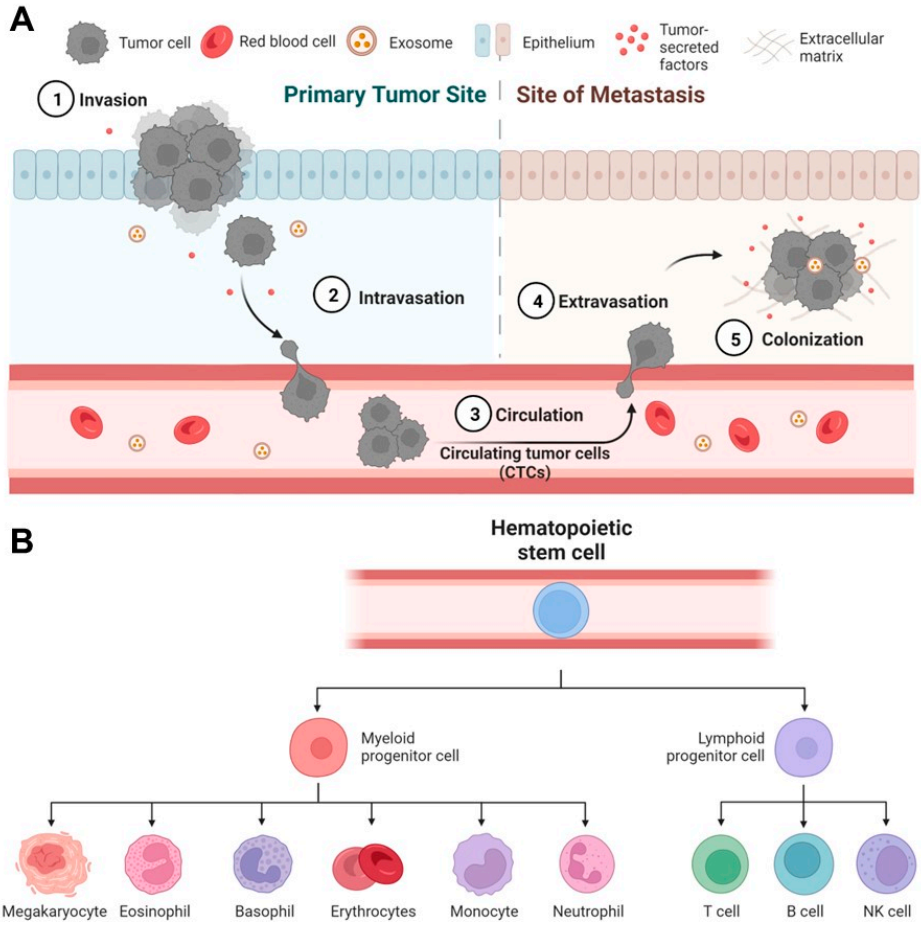

Figure 1. Rare cell-mediated bioprocesses in disease progression and tissue regeneration. (**A**) Circulating tumor cells (CTCs) play a critical role in cancer metastasis. In primary tumor sites, some highly invasive cancer cells undergo intravasation to enter the blood circulation and become CTCs. CTCs travel to distal organs and tissues, undergo extravasation, and eventually form deadly metastatic colonies. (**B**) Human hematopoietic stem/progenitor cells (HSPCs) have the potential to regenerate all types of blood cells. Under proper conditions in vitro and in vivo, HSPCs can differentiate into all myeloid (monocytes, neutrophils, etc.) and lymphoid cell lineages (T cells, B cells, etc.).

3. Pre-Requisition of Micro-Magnetofluidics: Labeling and Characterization

Magnetic labeling refers to the specific binding of magnetic nanobeads and target cells. Magnetic beads are usually conjugated with antibodies specific to the target cells (Figure 2A). To achieve magnetic separation, the magnetic loading of target cells is important. First, it requires high expression of certain antigens/proteins on the surface of target rare cells while low expression of such proteins on other cells. Choosing a good biomarker with high specificity for the target cells is essential for efficient magnetic separation. For example, EpCAM/cytokeratin, HER2, and vimentin have been used as biomarkers for CTCs and have shown great promise in differentiating CTCs from blood cells [23,82,83]. Other

than antibodies, aptamers have also been used for enhanced magnetic labeling [84–86]. Aptamers are single-stranded DNA or RNA that can specifically bond to target proteins and form DNA-protein entangled 3D structures. Aptamers can be obtained through the systematic evolution of ligands by Exponential Enrichment (SELEX) [87]. Compared with antibodies, aptamers have several advantages including high affinity, easy synthesis, and better stability [88]. As such, aptamer-decorated magnetic beads can bind better with surface markers on target cells compared with antibody-conjugated magnetic beads [88]. Additionally, the binding between aptamers and cell surface markers can be engineered to be reversible. It can facilitate the efficient release of magnetic beads after magnetic separation.

Magnetic beads are conjugated with antibodies in different ways. This can be through biotinylation, where magnetic beads coated with streptavidin are bonded with biotinylated antibodies [76,89,90]. This method is straightforward and can be easily implemented for magnetic labeling. Streptavidin usually has multiple binding sites for antibody conjugation. Therefore, it is also amenable for further decoration and forms magnetic bead conjugations and enhance magnetic signaling. However, in certain occasions, it can cause the clumping of target cells which can be unfavorable if single-cell collection is desired. Protein G and IgG interaction is another way for the conjugation of magnetic beads and antibodies. Magnetic beads are decorated with protein G which can be bonded with IgG. Such decoration allows a magnetic bead to be bonded with an antibody [91–93]. Therefore, the quantification of magnetic loading can be more accurate using magnetic beads with protein G. However, the binding between protein G and IgG can be less specific and less efficient compared with other bead conjugation methods. Antibodies covalently bonded to magnetic beads is a traditional method for antibody-bead conjugation [94]. It usually relies on the binding of carboxyl (COOH) group on the magnetic beads and the amine group on antibodies. Such binding is strong and irreversible and can significantly reduce the chance of bead detachment during magnetic sorting. However, this method is usually time-consuming and may cause loss of function of antibodies during a covalent binding reaction. To address these issues, optimized bead conjugation protocols have been proposed such as the Invitrogen Cross-Linking Immunoprecipitation (CLIP) Protocol. Other magnetic components were also proposed for magnetic labeling. For example, David Arnold et al. reported magnetic microdiscs for magnetic labeling of target cells and enhanced magnetic separation [95]. The magnetic susceptibility of magnetic beads can also be designed by adjusting the percentage of ion oxide (Fe_3O_4 or Fe_2O_3). Using different types of magnetic beads with varying ion oxide supplemented can achieve multiplexed cell separation. For example, Di Carlo et al. reported a magnetic ratcheting cytometry system that can separate $CD4^+$ T cells and $CD8^+$ T cells from the same blood samples by conjugating the two types of cells with magnetic beads containing different ion oxide levels [96].

The magnetic labeling of cells is commonly performed by simply mixing the cells with magnetic beads/discs in a small volume of buffer (e.g., 100 µL of phosphate buffered saline, PBS) for a short period (e.g., 10–30 min). Interestingly, a recent study suggested that this short period of time is sufficient for some cell types, for example, human T cells, to internalize some of the magnetic particles into cytoplasm and maintained the particles for 2 weeks [97]. In addition, the internalization of magnetic particles is reported to be size dependent [98]. Smaller particles generally underwent fast internalization. As iron particles have been reported to have dose-dependent cytotoxicity [99], it is highly desired to develop a new strategy to inhibit particle internalization during magnetic labeling, or at least perform a titration on labeling time to minimize the labeling time to reduce internalization [33].

To obtain the best performance of magnetic separation, it requires optimal magnetic loading on target cells. This is usually achieved by saturating magnetic binding between target cells and magnetic bead–antibody complexes. Measuring the magnetic mobility of magnetic labeled target cells is one way to determine the magnetic saturation of the target cells. Cell Tracking Velocimetry is used to measure the magnetic mobility of magnetic labeled target cells [100]. For this method, target cells are first saturated with antibodies

determined by flow cytometry. Magnetic beads specific to the antibodies were then supplemented to determine the saturation magnetic loading by measuring the cell movement in set incoming flow conditions.

Post magnetic labeling, magnetically labeled cells can be separated through macroscale magnetic columns [101]. This process is often referred to as magnetic-activated cell sorting (MACS) [102]. Over the years, a range of MACS-based products and systems have been commercialized for cell isolation, purification, and analysis. Although MACS has been widely used in research and clinical studies, it still has certain limitations, including low controllability and poor performance on weakly expressed markers [103,104]. Microfluidics-based magnetic sorting technologies become more appealing. It is not only amenable for a high level of controllability, but also sensitive enough for the separation of cells with extremely low magnetic susceptibility. Therefore, microfluidics-based magnetic separation generally performed better than off-the-shelf MACS technology and has enabled high-throughput, high-precision sorting of rare cells for diagnosis and therapeutics.

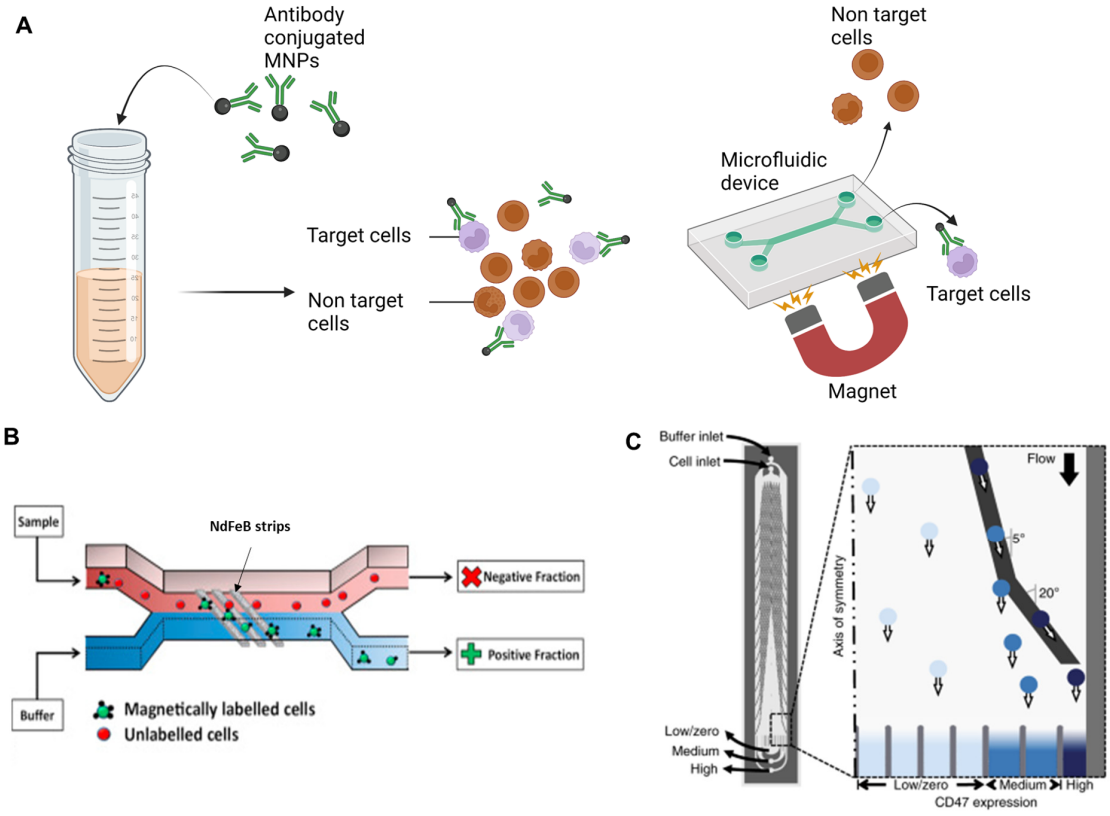

Figure 2. Working principle of magnetic deflection. (**A**) Illustration of magnetic labeling of target cells in cell mixture and magnetic sorting of target cells in the microfluidic device. (**B**) Illustration of magnetic deflection. Target rare cells were specifically labeled with antibody-conjugated magnetic nanoparticles. The sample mixture was then introduced to the microfluidic device. Target rare cells were then deflected due to the strong magnetic gradient produced by the ferromagnetic guide imbedded under the microchannel. Image reproduced with permission from [105]. Copyright 2017 Elsevier. (**C**) The PRISM device developed in the Kelley group. Magnetic guides made of metglas were branched out from the middle to the side of the microchannel. The magnetic guides have multiple incline angles with reference to the flow direction. Magnetically labeled rare cell thus experience different magnetic forces along the flow direction. Cells expressing different levels of biomarkers were then separated in different outlets. Image reproduced with permission from [106]. Copyright 2019 Nature Publishing Group.

4. Micro-Magnetic Deflection

4.1. Principles

Magnetic deflection is a main approach of magnetophoresis. It relies on the dictated movement/migration of target cells to achieve separation (Figure 2A). The main procedures of magnetic deflection include the specific magnetic labeling of target cells, the incorporation of an external magnetic field, and on-chip magnetic sorting.

The magnetic deflection of target cells is the result of interaction between magnetic force and hydrodynamic force on the cells. In the presence of an external magnetic field, magnetically labeled cells experience a magnetic force produced by the inserted magnetic gradient. In the meantime, the cells experience Stoke's drag force from the fluid flow. The magnetic force given as

$$\boldsymbol{F}_m = nV_{bead}\frac{\Delta\chi_{bead}}{\mu_0}(\boldsymbol{B}\cdot\nabla)\boldsymbol{B} \quad (1)$$

where n is the number of magnetic beads bound to the target cell, V_{bead} is the volume of a nanobead, $\Delta\chi_{bead}$ is the relative magnetic susceptibility of nanobeads, μ_0 is the magnetic permeability of the free space, and $\boldsymbol{B}$ is the magnetic field.

The drag force is expressed as

$$F_d = 6\pi\eta RU \quad (2)$$

where η is the viscosity of the ambient fluid, R is the radius of the t cell, and U is the velocity magnitude of the target cells relative to the flow.

To dictate magnetic deflection, both magnetic force and hydrodynamic force can be designed based on applications. For magnetic force manipulation, the magnetic labeling of target cells and magnetic gradient in the microchannel can be designed. The optimization of magnetic labeling was discussed above. The change in magnetic gradients can be achieved by modifying the magnetic field. For the optimization of hydrodynamic force, the flow pattern in the microchannel can be designed.

4.2. Magnetic and Hydrodynamic Optimization

The design of magnetic field is an important aspect for the optimization of magnetic deflection. To achieve a good deflection, a large magnetic gradient is required. To increase the magnetic gradient, researchers have tried different types of permanent magnets and different ways to place the magnets. The easiest strategy is to apply a macroscale permanent magnet on the side or at the bottom of the microfluidic device to produce magnetic gradient [107–109]. Target cells will be deflected due to the non-uniform magnetic field produced by the permanent magnet. However, the magnetic gradient may not be strong enough to achieve high-resolution magnetic deflection when target cells have low magnetic susceptibility. Alternatively, magnetic blocks arranged with opposing poles were used for a larger magnetic field gradient [110,111]. Micro-magnet arrays have also been applied to create strong local magnetic gradients to increase magnetic deflection sensitivity [112,113].

Insertion of paramagnetic materials has also been used to further enhance local magnetic gradients in the microfluidic device. Soft magnetic materials such as nickel and ion oxide micro- or nanostructures were integrated in microfluidic devices to create strong local magnetic gradients in the microchannel [105,114–116]. Tom Soh et al. have designed nickel microchannel strips to deflect magnetic labeled rare cells [117]. The magnetic ratcheting cytometry system developed by the Di Carlo group also applied soft magnetic materials for magnetic field enhancement and adjustment. In this system, micropillars made of soft materials were arranged at various distances to create multiple magnetic ratcheting zones in the sorting chamber. Periodically switching magnetic fields were produced under the microchip through rotating permanent magnets. The micropillars activated by the switching magnetic field drove magnetically labeled cells across the sorting chamber, and cells with different magnetic loading levels would be stabilized at different ratcheting zones [118,119]. In recent years, the Kelley group has developed a magnetic deflection-

based microfluidic chip-termed PRISM (Figure 2B) [106,120,121]. This system made use of the superb ferromagnetic property of an amorphous metal alloy ribbon called metglas to produce an extremely strong local magnetic field when external magnets were introduced. Through lithography and wet etching, metglas-based magnetic guide could be patterned on a glass substrate. SU8-based microchannels were then generated on top of the magnetic guide for sample processing and magnetic deflection. The magnetic guides embedded under the microchannel were designed to branch out from the middle to the sidewall of the microchannel with multiple magnetic deflection angles. Magnetically labeled rare cells were thus segregated into different subpopulations when following the magnetic guides.

Making use of hydrodynamic force is another way to dictate magnetic deflection. For example, designing microstructures in the microchannel to produce a low drag force zone can be used to isolate magnetically labeled cells for single-cell analysis [122]. Using different materials for channel substrates and optimized channel shapes to obtain uniform flow profiles is another way for drag force manipulation [123]. A third way is to introduce 'flow pockets' on the side the microchannel and apply permanent magnets along the 'flow pockets' [124,125]. The flow velocity is close to zero in the 'flow pockets' and non-target cells flowing along the fluid flow will not enter the 'flow pockets', while magnetic labeled target cells will be deflected and trapped in the 'flow pockets'. Table 1 summarizes different magnetic sorting methods and their relevant performance including throughput, target cell isolation efficiency, purity, sensitivity and their potential limitations.

Due to the miniaturized channel scale and strong inserted external magnetic field, microfluidics-based magnetic deflection can bring high deflection efficiency of target cells with good purity [14,126–128]. Additionally, since magnetically labeled cells move continuously along the sorting chamber, deflected target cells can be easily collected in the designated outlet with few cell loss. However, this method solely depends on magnetic force added on the target cells, which may not be enough to address the heterogeneity of target cells. Rare cells such as CTCs are known to be heterogenous in both biological and physical properties [129,130]. For example, CTCs undergoing epithelial to mesenchymal transition (EMT) will lose the expression of EpCAM [131–134]. Targeting EpCAM alone cannot isolate CTCs with low EpCAM expression. To address this problem, researchers introduced multiplex marker targeting [135–137]. In addition to EpCAM, biomarkers such N-cadherin, vimentin were used to differentiate CTCs under EMT from blood cells [138,139]. Alternatively, magnetic deflection can be combined with physical-property based cell separation methods to achieve superb CTC isolation efficiency.

Table 1. Comparison of different magnetic deflection-based cell sorting strategies.

Sorting Strategy	Application	Throughput	Efficiency	Purity	Sensitivity	Limitation	Reference
Magnetic guided deflection	CTC and CTC cluster isolation	0.5 mL/h	~90%	5.7 log white blood cell depletion	10 targe cell per mL	Strong cell–cell interaction at high cell concentration can affect its performance	[120]
Modified magnetic beads	Separation of cancer cells	NA	~90%	>80%	10^6 cells /mL	Large bead size reduce sensitivity	[140]
Captured magnetic bead-bounded target cells with dead-ended side chambers near the a permanent magnet	CTC isolation from whole blood	1.2 mL/h	>90%	<0.4% white blood cell capture	2–80 target cells spiked in 1 mL of blood	Lack of clinical sample processing	[108]

Table 1. *Cont.*

Sorting Strategy	Application	Throughput	Efficiency	Purity	Sensitivity	Limitation	Reference
Magnetophoresis assisted cell capture activated by magnet arrays	Isolation of cancer cells spiked in human blood	7.2 mL/h	>60%	~30%	3.5×10^4 cancer cells spiked in 1 mL of blood	Release of the rare cells would be challenging	[110]
Two-stage magnetic separation	White blood cell sorting from whole blood	1.2 mL/h	93%	>70%	10^3 cells/min	Require further optimization of rare cell separation	[114]
Ferromagnetic guide based deflection in a large scale 3D printed system	Isolation of mature natural killer cells from blood	>18 mL/h	>50%	~90%	10^7 cells per mL	Complicated fabrication and assembly process	[121]
Magnetic deflection facilitated single-cell capture	Capture of rare tumor cells from mouse blood	2 mL/h	~90%	>90%	<100 CTCs from 1 mL of whole blood	The system can be saturated due to the limited number of trap units	[122]
Magnetic deflection and capture on wavy-herringbone structures	Capture CTCs from whole blood	0.54 mL/h	92%	91%	100 target cells per mL blood	Lack of clinical processing	[125]
Magnetic ratcheting	Profiling of magnetically labeled immune cells in spiked samples	NA	87%	95%	10^7 cells per mL	The throughput was limited as no in-flow allowed during magnetic ratcheting	[118]

4.3. Fabrication of Magnetic Deflection-Based Microfluidic Devices

The functioning of magnetic deflection-based microfluidic devices requires two main components: microchannel/sorting chamber assembly and magnetic component combination. For most designs, the sorting chamber for magnetic deflection is integrated to the microchannels for sampling. Polydimethylsiloxane (PDMS) is the most common material for channel fabrication as it is transparent, air permeable, and biocompatible. PDMS substrates with microchannel/sorting chamber features can be conveniently fabricated using soft lithography [141]. Briefly, a mold such as a silicon master containing the channel features can be first fabricated using photolithography, and then liquid PDMS mix (base: curing agent = 10:1) is casted on the mold and polymerized at 70 °C for 2 h. The PDMS substrate is then bonded with a cover (e.g., a thin glass slide) to form the microchannel. Other than PDMS, other materials such as negative photoresist (e.g., SU8) were also used in channel fabrication [120]. SU8 channels can be fabricated through photolithography. For the integration of magnetic components, it can be direct integration by simply applying a permanent magnet at the top/bottom or on the side of the microchannel. It can also be a complicated process by adding soft magnetic materials. For the insertion of soft magnetic materials, there are multiple ways. The soft magnetic material can first be mixed in solution and then introduced to the bottom substrate of the device through injection molding [105]. Another way is to use wet etching to generate magnetic deflection features. For this method, the soft magnetic materials are first coated on the device substrate through electron beam physical vapor deposition or epoxy taping [120,142]. The soft magnetic layer is then patterned through wet etching masked by a photoresist layer. A third way

to generate soft magnetic features is through electroplating [118]. Different fabrications have pros and cons. For example, liquid soft magnetic material injection can plate magnetic materials easily, but it requires a mold with mirochannels for injection. Therefore, the shape and size of soft magnetic features can be limited. Deposited magnetic features can be highly accurate, but the thickness and magnetic strength of the material can be limited. For the taping of ferromagnetic material such as metglas, it can introduce an extremely strong local magnetic field. However, the taping process limits the smoothness of the substrate surface. Electroplated magnetic features can be generated with relatively high aspect ratio and brings strong local magnetic field. However, the resolution of electroplated feature is relatively low. As such, the fabrication methods chosen usually depends on the specific application of the microfluidic device.

4.4. Integration and Applications for Rare Cell Capture

Different approaches have been reported to combine magnetic deflection with other cell separation mechanisms, showing high compatibility of magnetic deflection. The integration of label-free cell sorting methods and magnetic deflection was widely explored since it usually shows advantages of both approaches. Label-free cell sorting methods generally give high throughput, while magnetic deflection shows high specificity. Toner et al. have developed an integrated microfluidic system that includes deterministic lateral displacement (DLD), inertial focusing and magnetic separation (Figure 3A) [26]. This system was able to isolate CTCs from untreated whole blood, where nucleated cells were first separated from red blood cells (RBCs) through DLD, followed by magnetic depletion of magnetically labeled white blood cells (WBCs). Since RBCs are significantly smaller than nucleated cells, DLD can separate nucleated cells from RBCs with high purity. Inertial focusing re-aligns nucleated cell mixture into single-cell strips which reduces the cell–cell interaction. Therefore, in the last step, the magnetic depletion of WBCs brought high CTC efficiency and purity. Similarly, Nasiri et al. presented a hybrid device combing inertial focusing and magnetic deflection for CTC isolation (Figure 3B) [143]. High isolation efficiency and purity can also be achieved. Several groups have combined dielectrophoresis (DEP) with magnetic separation for rare cell separation (Figure 3C) [144–146]. Nucleated cells were separated by size using DEP and target cells were then isolated through magnetic deflection. Combing magnetic deflection with acoustic-based sorting for the isolation of rare cells from whole blood was also widely studied [147]. Acoustics is a technology used for separating particles/cells based on the acoustic force which is proportional to the size of cells. As such, acoustics can also be used for the pre-sort of nucleated cells when integrated with magnetic deflection. Several other mechanisms incorporated with magnetic deflection were also reported to be highly efficient. For instance, Alipanah et al. developed a rare cell sorter using induced charged electroosmotic flow and magnetophoresis [148]. Shamloo et al. presented a system combining centrifugal force with magnetic deflection for efficiency and high-purity isolation of rare cells [149]. Javanmard et al. described a novel approach for the rapid assessment of surface markers on cancer cells using a combination of immunomagnetic separation and multi-frequency impedance cytometry. In this work, multi-frequency impedance cytometry was applied for target cell detection rather than separation [150].

Overall, the combination of magnetic separation with other cell separation methods can provide a more flexible and effective approach to isolate and purify specific cell populations. Magnetic separation alone may not achieve complete separation of the target cells from non-target cells or impurities. By combining magnetic separation with other separation methods, it is possible to increase the purity of the target cells, resulting in a more homogeneous sample [151,152]. On the other hand, label-free cell isolation methods usually differentiate cells based on physical properties such as size, dialectical properties, and density. Such methods are not applicable in heterogeneous samples, where physical properties alone cannot differentiate rare cells and non-target cells [153,154]. Combining them with magnetic separation can improve the selectivity and specificity of the separation.

Magnetic separation can be a rapid and efficient method for capturing cells, and when combined with other methods such as fluorescence-activated cell sorting (FACS) or centrifugation, it can result in higher capture and separation efficiency. In some cases, the combination of magnetic separation with other methods can reduce sample loss, which can be especially important when working with limited sample volumes.

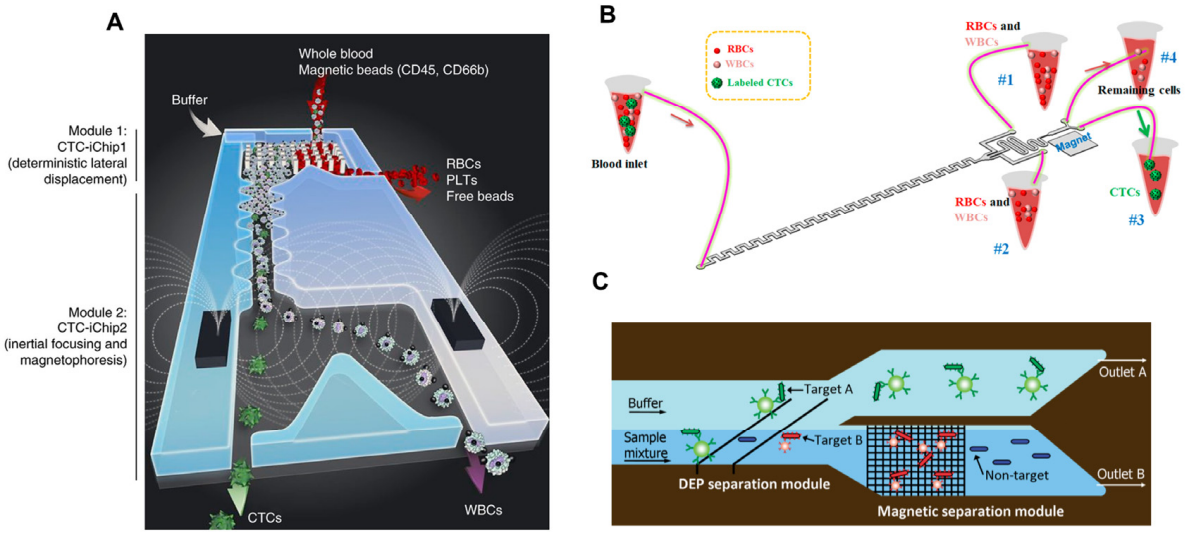

Figure 3. Integration of magnetic deflection with other rare cell isolation methods. (**A**) A microfluidic platform combing DLD, inertial focusing and magnetic deflection developed by Toner group. Image reproduced with permission from [26]. Copyright 2014 Nature Publishing Group. (**B**) Combition of inertial focusing and magnetic deflection. Image reproduced with permission from [143]. Copyright 2021 MDPI (**C**) Illustration of combining DEP and magnetic deflection for highly efficient cell sorting. Image reproduced with permission from [146]. Copyright 2009 Royal Society of Chemistry.

5. Micro-Magnetic Ranking

5.1. Principles and Fabrication

Magnetic ranking cytometry (MagRC) is another realization of micro-magnetofluidic cell capture proposed by Shana Kelley and co-workers in 2015 [155]. The core concept is also to balance the two major forces applied to the magnetically labeled cells present in a microfluidic channel—the magnetic force generated by the interaction between magnetic nanoparticles (MNPs) and permanent magnets, and the fluidic drag force generated by the fluids (Figure 4A) [155,156]. Once these two forces reach equilibrium, the cells will be captured in a specific capture region of the device, also referred to as the zones [157]. Compared to magnetic deflection, the key idea of MagRC to use microfluidic geometries to slow down the local fluidic profile so that the labeled cells with weakly magnetic labeling (equivalent to weakly expressed biomarkers) can be captured on-chip properly. In addition, for rare cell analysis, trapping rare cells on-chip helps the downstream quantitation process.

In the original article proposing MagRC, Mohamadi et al. tested five capture geometry and highlighted that the 'X'-shaped structures yielded the high-efficiency capture of cells [155]. Meanwhile, the 'X'-shaped structures also experienced minor levels of non-specific capture of non-magnetically labeled cells, such as WBCs. As benchmarked by Aldridge et al. [120], the 'X'-shaped capture pockets non-specifically trap 2000 WBCs per mL of blood, yielding a WBC depletion efficiency of 99.97% and outperforming other capture structures (e.g., Herringbone [125], 7000 WBCs per mL of blood). However, given the rarity of CTCs (a few cells in a million of WBCs), it is still necessary to perform optimization on the capture geometry used in MagRC to further reduce non-specific capture.

Upon capture, the target cells will remain stable on-chip for various downstream assays, including in situ microscopy [158], phenotypic assay [159], and cell culture [35]. Notably, similar to magnetic ratcheting cytometry, MagRC can fine-tune the local magnetic

fields and/or local fluidic velocity to enable not only the capture but also the quantitative profiling of rare cells based on a single marker, for example, EpCAM. This gives the researchers the ability to better understand the molecular profile of captured rare cells, which has been highlighted to be useful for disease monitoring and treatment decision-making. For example, recent studies have revealed that moderate-affinity T-cell receptors (a surface protein that governs tumor reactivity), rather than high or low affinity, drive the T cells to develop into mature memory T cells without significant dysfunction.

In practice, the workflow of MagRC takes approximately 2 h to complete and can be largely divided into three steps: magnetic labeling, microfluidic sorting, and downstream application (Figure 4B) [160]. In brief, a cell mixture containing rare cells are labeled by MNP-conjugated antibodies targeting a specific surface protein biomarker expressed specifically on the cellular membrane of the target cells, for example, EpCAM on CTCs or CD34 on HSPCs. Labeled cells are introduced into the microfluidic device with the 'X'-shaped capture pockets. The microfluidic device is sandwiched by arrays of neodymium permanent magnets (N52 grade) to generate stable external magnetic fields during device operation. The microfluidic sorting begins with withdrawing labeled cell mixture into the microfluidic device under a constant flow rate generated by a programmable syringe pump, often approximately 2–30 mL/h depending on the expression level of target proteins. Post the capture, cell-free washing solution will be introduced to the microfluidic device 2–3 times at the same flow rate to flush out the non-labeled cell population into the syringe reservoir. The captured rare cells will remain in the capture pocket based on the capture theory explained in the previous paragraph. At this time point, the captured rare cells can be treated differently to fulfill the demands of downstream assays. In some cases, the cells are fixed and permeabilized under a lower flow rate for on-chip immunostaining, followed by fluorescence microscopy. In other cases, external magnets are removed from the chips, and the cells are recovered from the chips at a higher flow rate to a different reservoir. Recovered cells are highly viable and suitable for most molecular and phenotypic assays, such as sequencing, flow cytometry, and direct culture. It is worth mentioning that the typical shear stress generated during the cell recovery process of MagRC is relatively small (<0.01 Pa) [72], which explains why sensitive cell types, such as cardiomyocytes and induced pluripotent stem cells, grew well post recovery [161].

The fabrication of MagRC can be carried out in a standard cleanroom setup [155]. First, photolithography is used to generate 'X'-shaped captured pockets on photoresist-coated silicon wafers. The patterned wafers are subsequently used as a mold for soft-lithography to generate polydimethylsiloxane (PDMS) chip replicas. PDMS replicas are plasma bonded to a thin glass coverslip to finish the chip. As the chip design contains multi-depth structures, the fabrication involves multiple-step mask alignment and photolithography, which makes the cleanroom-based procedure complicated and time-consuming. Alternatively, high-resolution stereolithography can be utilized to generate the mold for PDMS casting via one-step 3D printing [161]. The use of 3D printing greatly simplified the mold generation process. However, the microstructure generated by 3D printing is a bit rough compared to standard photolithography [35,161]. The impact of suboptimal capture pockets on capture performance is not well studied at this moment and may deserve further investigation.

5.2. Applications

Since its first release in 2015, Kelley and co-workers paid a substantial effort to demonstrate the utility of MagRC for rare cell capture, isolation, characterization, and expansion. They firstly highlighted that the MagRC device can be used to track the expression level of EpCAM on rare CTCs and the expression profile of EpCAM correlated to the progression of tumor metastases (Figure 5A) [155,156]. In these studies, they demonstrated the value of quantitative profiling of CTCs and reported that not only the number of CTCs, but also the EpCAM level of CTCs, predict the metastatic status in late-stage prostate cancer patients. Higher averaged zonal number, or equivalently lower expression of EpCAM, correlated with disease progression [156]. Later on, they demonstrated that the MagRC system is

useful for studying tumor precursor cells (Figure 5B) [162]. In this study, Duong et al. used MagRC to capture rare mesothelin (MSLN) -expressing cells in blood circulation and studied the expression of CD34 and CD90 on captured mesothelioma precursor cells. It was found that $MSLN^+CD90^+$ cells are largely present in the early stage (asbestos-exposed) patients while $MSLN^+CD34^+$ cells are present in the late stage (advanced mesothelioma, Figure 5B). This is the first study to reveal the prognostic importance of $MSLN^+CD90^+$ and cells in the early diagnosis of mesothelioma. There are also practices to combine MagRC with other microfluidic or molecular approaches for the comprehensive characterization of CTCs and tumor precursor cells. For example, Poudineh et al. combined MagRC with the chemokine-mediated migration assay to simultaneously characterize the mobility of isolated CTCs [163]. Green et al. recovered CTCs from the MagRC and performed the collagen uptake assay by culturing recovered live CTCs for up to 48 h to assess the invasion behavior of isolated CTCs [159]. Lastly, at this moment, MagRC has advanced to the pre-clinical study stage and demonstrated that the number and EpCAM status of captured CTCs are valuable prognostic biomarkers for metastatic prostate cancer using a cohort containing 36 patients [36]. Taken together, these studies highlighted the value of MagRC as a powerful device for cancer liquid biopsy.

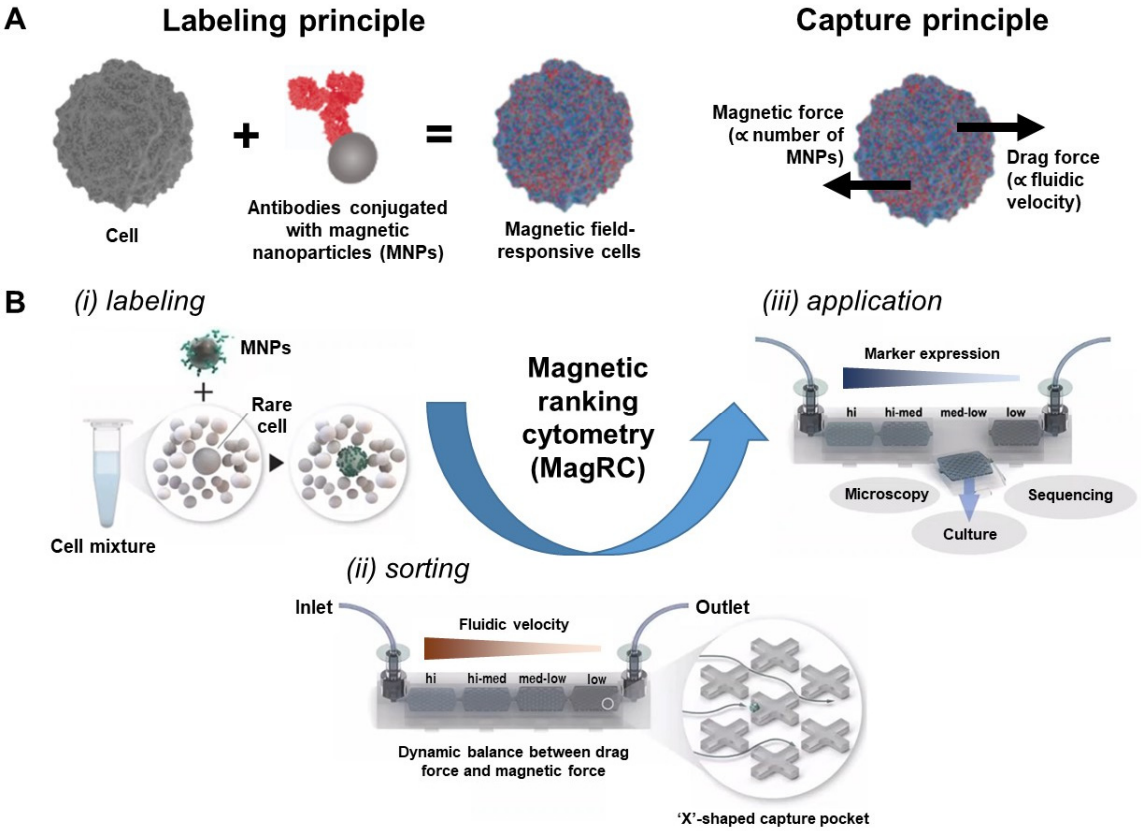

Figure 4. Principle and workflow of magnetic ranking cytometry (MagRC). (**A**) MagRC relies on magnetic labeling and microfluidics-mediated capture. Target cells were labelled by antibodies conjugated with MNPs to become responsive to external magnetic fields. When introduced into the microfluidic device, the magnetically labeled cells experienced two types of major forces—the magnetic force and the drag force. The cells will be captured once these two forces reach equilibrium. (**B**) MagRC involves three major procedures during operation: (i) labeling, (ii) sorting, and (iii) downstream application. Image reproduced with permission from [160]. Copyright 2020 American Chemical Society.

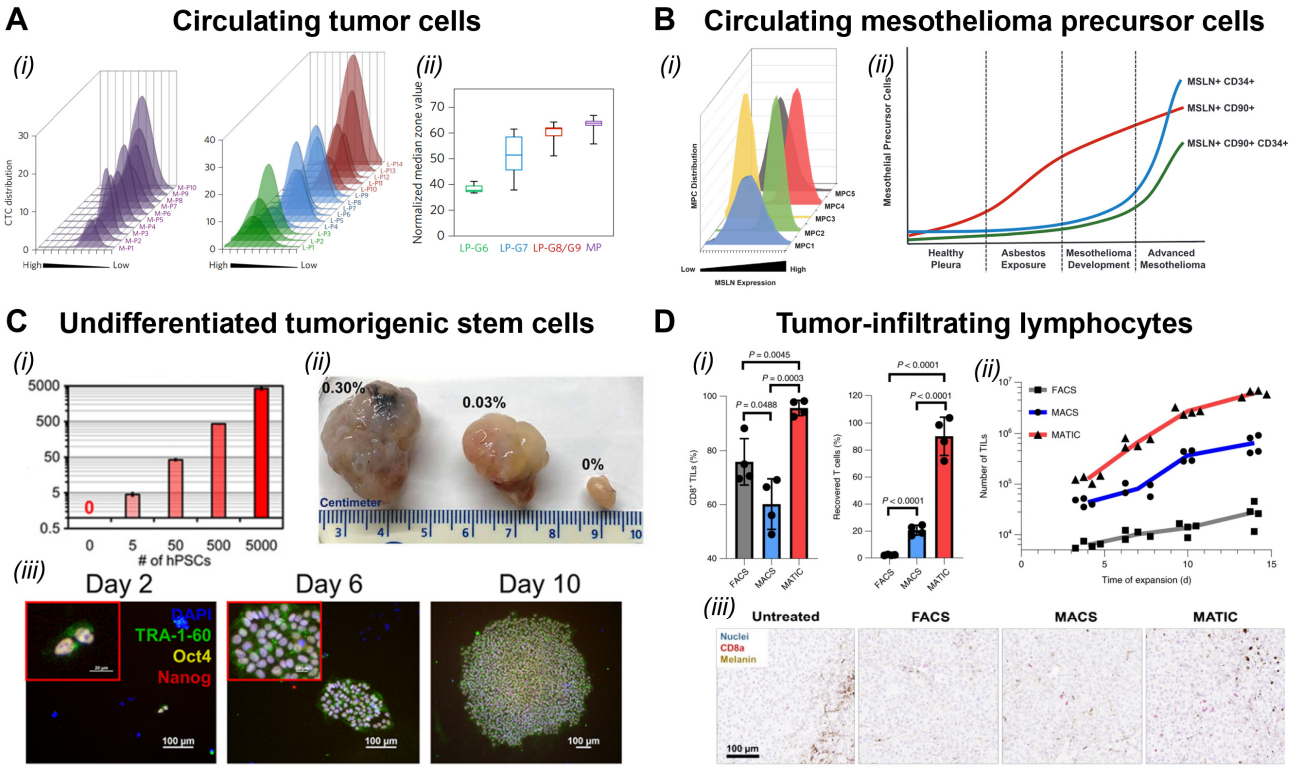

Figure 5. Applications of MagRC in capturing rare cells for disease diagnosis and therapeutics. (**A**) MagRC-mediated capture of CTCs. (i) EpCAM-based CTC profiles from patients with metastatic prostate (MP, purple) and localized (LG) prostate tumors. Patients with Gleason score of 6, 7, and 8–9 were in green, blue, and red, respectively. (ii) Box plot indicating the median zone values of the captured CTCs. More severe disease resulted in higher number of CTCs and lower EpCAM expression. Image reproduced with permission from [156]. Copyright 2017 Nature Publishing Group. (**B**) MagRC-mediated capture of circulating mesothelioma precursor cells (MPC). (i) Mesothelin-based MPC profile from patients with mesothelioma. (ii) Illustration of MPC subtypes and their typical marker expression derived from the captured rare cells. Image reproduced with permission from [162]. Copyright 2020 Elsevier. (**C**) MagRC-mediated capture and recovery of tumorigenic stem cells. (i) Capture performance of TRA-1-60-based capture of rare pluripotent stem cells. MagRC can robustly detect five rare stem cells spiked in 1 million non-target cells, yielding a limit of detection of 0.0005%. (ii) Pictures of teratoma (stem cell-derived tumor) developed from 300 (0.03%) and 3000 (0.3%) rare pluripotent stem cells. (iii) Fluorescence images of live rare pluripotent stem cells recovered from MagRC post sorting. Isolated rare stem cells expressed typical markers of pluripotency (e.g., TRA-1-60, Oct4 and Nanog) and developed colony over 10 days of culture, demonstrating a strong viability and potency. Image reproduced with permission from [161]. Copyright 2020 American Association for the Advancement of Science. (**D**) MagRC-mediated capture and recovery of tumor-infiltrating lymphocytes (TILs). (i) MagRC (also referred as MATIC) offer high-purity, high-yield capture and recovery of TILs from dissociated tumor cells compared to other cell isolation approaches such as FACS and MACS. (ii) The high yield of MagRC resulted in better expansion rare of TILs. More than 5×10^6 TILs can be generated with 14 days of culture. (iii) Expanded TILs are highly potent in tumor infiltration as revealed by the immunohistochemistry images. Number of infiltrated TILs can be quantified by counting the $CD8^+$ (pink) dots. Image reproduced with permission from [35]. Copyright 2022 Nature Publishing Group.

MagRC has been applied to study rare cell populations present in therapeutic cells, such as the undifferentiated human induced pluripotent stem cells (hiPSCs) present in the differentiated cardiomyocyte populations for regenerative therapy (Figure 5C) [161]. In brief, rare undifferentiated hiPSCs present in the therapeutic population have the potential to form teratoma, a stem cell-derived cancer, after engraftment due to their ability to

actively proliferate and differentiate [67,68]. This resulted in a significant safety concern to the clinical administration of hiPSC-derived therapeutic cells [164,165]. It has been reported that even 0.03% of hiPSCs in the differentiated cells is sufficient to form a teratoma in immunocompromised animals [166] and therefore a sensitive technology is needed to accurately detect rare hiPSCs. Kelley and co-workers proposed an alternative version of MagRC for the precise quantitation of hiPSCs based on TRA-1-60, a strongly expressed pluripotency-related biomarker, and achieved a detection limit of 0.0005% (Figure 5C). They also performed animal studies to ensure this sensitivity is sufficient to predict the formation of teratoma in immunocompromised animals. Given its rapid assay time (~2 h) and unprecedented sensitivity, MagRC has a high potential to become a standard assay for assessing the contamination of rare hiPSCs in therapeutic cells. In addition to the detection, MagRC can be used to refine the therapeutic cells based on their surface markers. In a recent study, Kelley and co-workers designed a high-throughput version of MagRC that supports the sorting of 3.2 billion cells per hour and used this system to purify highly potent tumor-infiltrating lymphocytes (TILs) from bulk preparation (Figure 5D) [35]. This approach is named microfluidic affinity targeting of infiltrating cells (MATIC). During the process, billions of TILs were sorted based on the expression of CD8 and/or CD39, a surface biomarker that indicates the level of activation and exhaustion of T cells. Compared to other cell sorting approaches such as FACS and MACS, MATIC resulted in much higher purity and yield rate post sorting, thanks to the high level of controllability of parallelization of microfluidics. The high purity and yield accelerated the vein-to-vein turnaround time of TIL therapy and improved the overall therapeutic outcomes, as measured by the level of TIL infiltration and median survival days of animals (Figure 5D).

The use of MagRC has also allowed new types of rare cells to be identified. A recent article reported the discovery of circulating tumor-reactive lymphocytes (cTRLs) in peripheral blood with the help of MagRC [167]. This cell type, although present in blood circulation, is tumor-specific and could kill autologous tumors and metastases effectively post expansion. As a result, this cell type holds great promise for the development of next-generation adoptive cell therapies against cancer metastases. Interestingly, a simple MagRC procedure [167] and a complicated FACS + scRNA sequencing procedure [168] resulted in the discovery of the same biomarker (CD103) of the cTRL population. This showcases the high fidelity of MagRC in rare cell analysis. Besides, MagRC is also compatible with non-cell targets. For example, Chang et al. recently published a study using MagRC for ranking magnetically labeled polystyrene beads for biomolecular display and selection [169], demonstrating the good versatility of MagRC as a general platform for bioseparation.

In addition to the efforts of Kelley and co-workers, other researchers also implemented the concept of MagRC to detect rare cells for diagnosis and therapeutics. For example, Noosawat et al. desgiened V- and W-shaped nicket microstructures to capture malaria-infected red blood cells that have increased magnetic susceptibility [170]. They achieved 80% capture efficacy of infected mouse blood with a 200 μm × 200 μm × 40 μm capture pockets, though no significant difference between V- and W-shaped microstructures was observed. In addition, Descamps et al. deposited NdFeB microparticles into microfluidic channels to form magnetic micropillars for capturing circulating tumor cells [171]. The system was designed to trap small WBCs on-chip effectively while allowing CTCs to pass through. The system achieved a depletion efficacy of up to 85% for WBCs, allowing CTCs to be purified for downstream culture and molecular assays.

6. Outlook

At this moment, two major challenges need to be addressed to further translate the micro-magnetofluidics from bench to bedside. The first challenge is the capability for multi-marker isolation and analysis. It is well acknowledged that the CTC populations contain a high level of heterogeneity [172–174]. We are unlikely to discover a one-for-all biomarker for CTC capture. Indeed, multiple articles have reported that a subpopulation of CTCs may undergo a complete epithelial-to-mesenchymal transition (EMT) and become EpCAM

negative in breast [175], lung [176], and colorectal [177] tumors. Therefore, EpCAM, the current 'universal' marker for CTCs is potentially biased and may not reflect the whole landscape of metastasizing cells [178]. Multiple alternative biomarkers have been proposed to facilitate the capture and analysis considering the EMT nature of CTCs such as Vimentin [179], N-Cadherin [180], AR-V7 [181], HER2 [182], and Ki67 [183]. These markers are generally overexpressed on CTC subpopulations and are highly associated with the mesenchymal phenotypes of cancer cells [184]. However, these markers are also expressed in normal mesenchymal cells that are irrelevant to metastasis, such as circulating fibrocytes ($Vimentin^{+}CD34^{+}$) [185]. Hence, there is an urgent need to develop magnetic sorting technology that is able to sort on the basis of multiple markers (e.g., EpCAM, vimentin, and CD34) for the accurate phenotyping of CTCs.

Unfortunately, unlike fluorescence signals, we do not have a spectrum of magnetic interactions. Hence, most of the current approaches perform multi-marker magnetic sorting on a serial (one-by-one) basis [163,186], which is extremely time-consuming and operationally complicated. It will be interesting to design new strategies that allow magnetic sorting to be performed based on the expression of multiple biomarkers simultaneously. Soh and co-workers proposed using magnetic beads with significantly different dimensions to generate size-dependent magnetic deflection and had success in separating bacterial cells [142]. This idea is interesting and may be worth further exploration. There might be a possibility to develop new stimulus-responsive magnetic materials based on the inverse Faraday effect [187], or develop a new bead hierarchy that can be decoupled on microfluidic devices [188]. In addition, it might be possible to couple magnetically captured cells with other high-throughput microfluidic assays, such as aqueous droplets [189] or hydrogel droplets [190], for multiplexed rare cell analysis post capture. Di Carlo and co-workers recently demonstrated rare antibody-secreting B cells can be encapsulated into their hydrogel nano-vials and separated based on the level of secretion effectively [191,192].

In addition to the single-marker limit, the current micro-magnetofluidic devices have experienced difficulties in scale-up applications due to poor manufacturability. Indeed, the majority of the designs proposed above, such as Prism [120] and magnetic ratcheting cytometry [96], require the accurate assembly of micro-magnets with the corresponding fluidic channels. This requirement is difficult to be achieved during large-scale manufacturing at a reasonable cost, which greatly hampers their translation as affordable technologies for routine clinical applications. The MagRC devices do not require such fine assembly but need to generate complex, multi-depth structures in the fluidic channel, which is not easy to be fabricated through micro-molding. 3D printing may be served as an alternative given its capability to generate multi-depth structures [193–196]. However, the feasibility of 3D printing in large-scale fabrication (>10,000 pieces per month) remains to be verified [197–199].

Lastly, to further translate micro-magnetofluidic devices from bench-to-bed, one must consider their simplicity, integrity and ease of use. At this moment, the majority of micro-magnetofluidic devices reply on external syringe pumps and pressure sources for operation, and dedicated or even customized microscopes for visualization and performance tracking. It is highly desired to develop a simplified, all-in-one version of micro-magnetofluidic systems for diagnostic and therapeutic applications. Indeed, Di Carlo and Emaminejad groups recently reported an all-in-one ferrobotic system for accessible and automated viral testing [200], which provides an excellent model for integrating micro-magnetofluidic systems. In fact, multiple low-cost and accessible alternatives of pumps [201,202] and microscopes [203–205] have been developed in the last 10 years. Most of them were made with off-the-shelf components and are open source, and will therefore facilitate fast and easy integration with the current micro-magnetofluidic devices.

7. Conclusions

In summary, micro-magnetofluidic devices are promising solutions for the rapid and sensitive analysis of rare cells present in biofluids, such as peripheral blood and cell

suspension. Impressively, the inherent high throughput of micro-magnetofluidics has enabled the direct processing of whole-blood samples for CTC quantitation, enrichment, and analysis. The whole assay can be completed in a clinically relevant turnaround (a few hours), making it an excellent candidate for non-invasive cancer screening and monitoring. After 15 years of development, micro-magnetofluidic devices have generated encouraging outcomes in the laboratory. At this moment, we are well equipped with the technologies that allow us to find the right needles in haystacks. With multiple mature designs being tested at the preclinical and clinical stages, we are optimistic about the future of magneto-microfluidic assays as a standard procedure for the analysis of rare disease-related cells. We hope, in the next ten years, that the micro-magnetofluidic assays can be mass produced at a reasonable cost and widely implemented in the clinic.

Author Contributions: K.C. and Z.W. both contributed to literature review, writing, revision and proofreading of this manuscript. All authors have read and agreed to the published version of the manuscript.

Funding: Z.W. is supported by the Banting Postdoctoral Fellowship Program (Grant #: RN488902-489318) provided by the Canadian Institutes of Health Research.

Institutional Review Board Statement: Not applicable.

Informed Consent Statement: Not applicable.

Data Availability Statement: Not applicable.

Acknowledgments: The authors thank the support of Gan Li for making the writing of this review joyful.

Conflicts of Interest: Z.W. is a paid consultant of CTRL Therapeutics, a company utilizing magnetic ranking cytometry for cellular therapy development.

References

1. Roy, A.L.; Conroy, R.S. Toward mapping the human body at a cellular resolution. *Mol. Biol. Cell* **2018**, *29*, 1779–1785. [CrossRef]
2. Allan, A.L.; Keeney, M. Circulating tumor cell analysis: Technical and statistical considerations for application to the clinic. *J. Oncol.* **2010**, *2010*, 426218. [CrossRef]
3. Roederer, M. How many events is enough? Are you positive? *Cytom. A* **2008**, *73*, 384–385. [CrossRef]
4. Hedley, B.D.; Keeney, M. Technical issues: Flow cytometry and rare event analysis. *Int. J. Lab. Hematol.* **2013**, *35*, 344–350. [CrossRef]
5. Lopresti, A.; Malergue, F.; Bertucci, F.; Liberatoscioli, M.L.; Garnier, S.; DaCosta, Q.; Finetti, P.; Gilabert, M.; Raoul, J.L.; Birnbaum, D.; et al. Sensitive and easy screening for circulating tumor cells by flow cytometry. *JCI Insight* **2019**, *5*, e128180. [CrossRef] [PubMed]
6. Muchlinska, A.; Smentoch, J.; Zaczek, A.J.; Bednarz-Knoll, N. Detection and Characterization of Circulating Tumor Cells Using Imaging Flow Cytometry-A Perspective Study. *Cancers* **2022**, *14*, 4178. [CrossRef]
7. Bhagwat, N.; Dulmage, K.; Pletcher, C.H., Jr.; Wang, L.; DeMuth, W.; Sen, M.; Balli, D.; Yee, S.S.; Sa, S.; Tong, F.; et al. An integrated flow cytometry-based platform for isolation and molecular characterization of circulating tumor single cells and clusters. *Sci. Rep.* **2018**, *8*, 5035. [CrossRef]
8. Awasthi, N.P.; Kumari, S.; Neyaz, A.; Gupta, S.; Agarwal, A.; Singhal, A.; Husain, N. EpCAM-based Flow Cytometric Detection of Circulating Tumor Cells in Gallbladder Carcinoma Cases. *Asian Pac. J. Cancer Prev.* **2017**, *18*, 3429–3437.
9. Musina, A.M.; Zlei, M.; Mentel, M.; Scripcariu, D.V.; Stefan, M.; Anitei, M.G.; Filip, B.; Radu, I.; Gavrilescu, M.M.; Panuta, A.; et al. Evaluation of circulating tumor cells in colorectal cancer using flow cytometry. *J. Int. Med. Res.* **2021**, *49*, 300060520980215. [CrossRef]
10. Holzner, G.; Mateescu, B.; van Leeuwen, D.; Cereghetti, G.; Dechant, R.; Stavrakis, S.; deMello, A. High-throughput multiparametric imaging flow cytometry: Toward diffraction-limited sub-cellular detection and monitoring of sub-cellular processes. *Cell Rep.* **2021**, *34*, 108824. [CrossRef]
11. Stavrakis, S.; Holzner, G.; Choo, J.; deMello, A. High-throughput microfluidic imaging flow cytometry. *Curr. Opin. Biotechnol.* **2019**, *55*, 36–43. [CrossRef]
12. Chen, K.; Hugh Fan, Z. Introduction to Microfluidics. In *Circulating Tumor Cells*; Oxford University Press: Oxford, UK, 2016; pp. 33–50.
13. Chen, Y.; Li, P.; Huang, P.H.; Xie, Y.; Mai, J.D.; Wang, L.; Nguyen, N.T.; Huang, T.J. Rare cell isolation and analysis in microfluidics. *Lab Chip* **2014**, *14*, 626–645. [CrossRef]
14. Wyatt Shields, C., IV; Reyes, C.D.; López, G.P. Microfluidic cell sorting: A review of the advances in the separation of cells from debulking to rare cell isolation. *Lab Chip* **2015**, *15*, 1230–1249. [CrossRef]

15. Pratt, E.D.; Huang, C.; Hawkins, B.G.; Gleghorn, J.P.; Kirby, B.J. Rare Cell Capture in Microfluidic Devices. *Chem. Eng. Sci.* **2011**, *66*, 1508–1522. [CrossRef]
16. Smith, J.P.; Barbati, A.C.; Santana, S.M.; Gleghorn, J.P.; Kirby, B.J. Microfluidic transport in microdevices for rare cell capture. *Electrophoresis* **2012**, *33*, 3133–3142. [CrossRef]
17. Luo, T.; Fan, L.; Zhu, R.; Sun, D. Microfluidic Single-Cell Manipulation and Analysis: Methods and Applications. *Micromachines* **2019**, *10*, 104. [CrossRef]
18. Wang, Z.; Jin, X.; Tian, Z.; Menard, F.; Holzman, J.F.; Kim, K. A Novel, Well-Resolved Direct Laser Bioprinting System for Rapid Cell Encapsulation and Microwell Fabrication. *Adv. Healthc. Mater.* **2018**, *7*, e1701249. [CrossRef]
19. Wang, Z. Detection and Automation Technologies for the Mass Production of Droplet Biomicrofluidics. *IEEE Rev. Biomed. Eng.* **2018**, *11*, 260–274. [CrossRef]
20. Lam, E.H.Y.; Yu, F.; Zhu, S.; Wang, Z. 3D Bioprinting for Next-Generation Personalized Medicine. *Int. J. Mol. Sci.* **2023**, *24*, 6357. [CrossRef]
21. Wong, I.Y.; Javaid, S.; Wong, E.A.; Perk, S.; Haber, D.A.; Toner, M.; Irimia, D. Collective and individual migration following the epithelial-mesenchymal transition. *Nat. Mater.* **2014**, *13*, 1063–1071. [CrossRef]
22. Wang, Z.; Samanipour, R.; Kim, K. Organ-on-a-Chip Platforms for Drug Screening and Tissue Engineering. In *Biomedical Engineering: Frontier Research and Converging Technologies*; Springer: New York, NY, USA, 2016; pp. 209–233.
23. Nagrath, S.; Sequist, L.V.; Maheswaran, S.; Bell, D.W.; Irimia, D.; Ulkus, L.; Smith, M.R.; Kwak, E.L.; Digumarthy, S.; Muzikansky, A.; et al. Isolation of rare circulating tumour cells in cancer patients by microchip technology. *Nature* **2007**, *450*, 1235–1239. [CrossRef] [PubMed]
24. Chen, K.; Amontree, J.; Varillas, J.; Zhang, J.; George, T.J.; Fan, Z.H. Incorporation of lateral microfiltration with immunoaffinity for enhancing the capture efficiency of rare cells. *Sci. Rep.* **2020**, *10*, 14210. [CrossRef] [PubMed]
25. Varillas, J.I.; Chen, K.; Zhang, J.; George, T.J., Jr.; Hugh Fan, Z. A Novel Microfluidic Device for Isolation of Circulating Tumor Cells from Pancreatic Cancer Blood Samples. *Methods Mol. Biol.* **2017**, *1634*, 33–53.
26. Karabacak, N.M.; Spuhler, P.S.; Fachin, F.; Lim, E.J.; Pai, V.; Ozkumur, E.; Martel, J.M.; Kojic, N.; Smith, K.; Chen, P.I.; et al. Microfluidic, marker-free isolation of circulating tumor cells from blood samples. *Nat. Protoc.* **2014**, *9*, 694–710. [CrossRef] [PubMed]
27. Labib, M.; Kelley, S.O. Single-cell analysis targeting the proteome. *Nat. Rev. Chem.* **2020**, *4*, 143–158. [CrossRef]
28. Yang, X.; Liu, W.; Chan, D.C.; Ahmed, S.U.; Wang, H.; Wang, Z.; Nemr, C.R.; Kelley, S.O. Fluorescent Droplet Cytometry for On-Cell Phenotype Tracking. *J. Am. Chem. Soc.* **2020**, *142*, 14805–14809. [CrossRef]
29. Tsao, S.C.; Wang, J.; Wang, Y.; Behren, A.; Cebon, J.; Trau, M. Characterising the phenotypic evolution of circulating tumour cells during treatment. *Nat. Commun.* **2018**, *9*, 1482. [CrossRef]
30. Wang, J.; Koo, K.M.; Wang, Y.; Trau, M. Engineering State-of-the-Art Plasmonic Nanomaterials for SERS-Based Clinical Liquid Biopsy Applications. *Adv. Sci.* **2019**, *6*, 1900730. [CrossRef]
31. Chai, S.; Ruiz-Velasco, C.; Naghdloo, A.; Pore, M.; Singh, M.; Matsumoto, N.; Kolatkar, A.; Xu, L.; Shishido, S.; Aparicio, A.; et al. Identification of epithelial and mesenchymal circulating tumor cells in clonal lineage of an aggressive prostate cancer case. *NPJ Precis. Oncol.* **2022**, *6*, 41. [CrossRef]
32. Gerdtsson, E.; Pore, M.; Thiele, J.A.; Gerdtsson, A.S.; Malihi, P.D.; Nevarez, R.; Kolatkar, A.; Velasco, C.R.; Wix, S.; Singh, M.; et al. Multiplex protein detection on circulating tumor cells from liquid biopsies using imaging mass cytometry. *Converg. Sci. Phys. Oncol.* **2018**, *4*, 015002. [CrossRef]
33. Wang, Z.; Wang, H.; Lin, S.; Ahmed, S.; Angers, S.; Sargent, E.H.; Kelley, S.O. Nanoparticle Amplification Labeling for High-Performance Magnetic Cell Sorting. *Nano Lett.* **2022**, *22*, 4774–4783. [CrossRef]
34. Lin, G. Magnetic particles for multidimensional in vitro bioanalysis. *View* **2021**, *2*, 20200076. [CrossRef]
35. Wang, Z.; Ahmed, S.; Labib, M.; Wang, H.; Hu, X.; Wei, J.; Yao, Y.; Moffat, J.; Sargent, E.H.; Kelley, S.O. Efficient recovery of potent tumour-infiltrating lymphocytes through quantitative immunomagnetic cell sorting. *Nat. Biomed. Eng.* **2022**, *6*, 108–117. [CrossRef] [PubMed]
36. Green, B.J.; Nguyen, V.; Atenafu, E.; Weeber, P.; Duong, B.T.V.; Thiagalingam, P.; Labib, M.; Mohamadi, R.M.; Hansen, A.R.; Joshua, A.M.; et al. Phenotypic Profiling of Circulating Tumor Cells in Metastatic Prostate Cancer Patients Using Nanoparticle-Mediated Ranking. *Anal. Chem.* **2019**, *91*, 9348–9355. [CrossRef] [PubMed]
37. Hejazian, M.; Nguyen, N.T. Magnetofluidic concentration and separation of non-magnetic particles using two magnet arrays. *Biomicrofluidics* **2016**, *10*, 044103. [CrossRef] [PubMed]
38. Nguyen, N.-T. Micro-magnetofluidics: Interactions between magnetism and fluid flow on the microscale. *Microfluid. Nanofluid.* **2012**, *12*, 1–16. [CrossRef]
39. Lenshof, A.; Laurell, T. Continuous separation of cells and particles in microfluidic systems. *Chem. Soc. Rev.* **2010**, *39*, 1203–1217. [CrossRef]
40. Yaman, S.; Anil-Inevi, M.; Ozcivici, E.; Tekin, H.C. Magnetic Force-Based Microfluidic Techniques for Cellular and Tissue Bioengineering. *Front. Bioeng. Biotechnol.* **2018**, *6*, 192. [CrossRef]
41. Pamme, N.; Wilhelm, C. Continuous sorting of magnetic cells via on-chip free-flow magnetophoresis. *Lab Chip* **2006**, *6*, 974–980. [CrossRef]

42. Frenea-Robin, M.; Marchalot, J. Basic Principles and Recent Advances in Magnetic Cell Separation. *Magnetochemistry* **2022**, *8*, 11. [CrossRef]
43. Proserpio, V.; Lonnberg, T. Single-cell technologies are revolutionizing the approach to rare cells. *Immunol. Cell Biol.* **2016**, *94*, 225–229. [CrossRef] [PubMed]
44. Dharmasiri, U.; Witek, M.A.; Adams, A.A.; Soper, S.A. Microsystems for the capture of low-abundance cells. *Annu. Rev. Anal. Chem.* **2010**, *3*, 409–431. [CrossRef] [PubMed]
45. Maheswaran, S.; Haber, D.A. Circulating tumor cells: A window into cancer biology and metastasis. *Curr. Opin. Genet. Dev.* **2010**, *20*, 96–99. [CrossRef] [PubMed]
46. Zhang, J.; Chen, K.; Fan, Z.H. Circulating Tumor Cell Isolation and Analysis. *Adv. Clin. Chem.* **2016**, *75*, 1–31.
47. Poudineh, M.; Sargent, E.H.; Pantel, K.; Kelley, S.O. Profiling circulating tumour cells and other biomarkers of invasive cancers. *Nat. Biomed. Eng.* **2018**, *2*, 72–84. [CrossRef]
48. Abouali, H.; Hosseini, S.A.; Purcell, E.; Nagrath, S.; Poudineh, M. Recent Advances in Device Engineering and Computational Analysis for Characterization of Cell-Released Cancer Biomarkers. *Cancers* **2022**, *14*, 288. [CrossRef]
49. Green, B.J.; Saberi Safaei, T.; Mepham, A.; Labib, M.; Mohamadi, R.M.; Kelley, S.O. Beyond the Capture of Circulating Tumor Cells: Next-Generation Devices and Materials. *Angew. Chem. Int. Ed. Engl.* **2016**, *55*, 1252–1265. [CrossRef]
50. Pantel, K.; Speicher, M.R. The biology of circulating tumor cells. *Oncogene* **2016**, *35*, 1216–1224. [CrossRef]
51. Woo, D.; Yu, M. Circulating tumor cells as "liquid biopsies" to understand cancer metastasis. *Transl. Res.* **2018**, *201*, 128–135. [CrossRef]
52. Alva, A.; Friedlander, T.; Clark, M.; Huebner, T.; Daignault, S.; Hussain, M.; Lee, C.; Hafez, K.; Hollenbeck, B.; Weizer, A.; et al. Circulating Tumor Cells as Potential Biomarkers in Bladder Cancer. *J. Urol.* **2015**, *194*, 790–798. [CrossRef]
53. Danila, D.C.; Fleisher, M.; Scher, H.I. Circulating tumor cells as biomarkers in prostate cancer. *Clin. Cancer Res.* **2011**, *17*, 3903–3912. [CrossRef] [PubMed]
54. Yap, T.A.; Lorente, D.; Omlin, A.; Olmos, D.; de Bono, J.S. Circulating tumor cells: A multifunctional biomarker. *Clin. Cancer Res.* **2014**, *20*, 2553–2568. [CrossRef] [PubMed]
55. den Toonder, J. Circulating tumor cells: The Grand Challenge. *Lab Chip* **2011**, *11*, 375–377. [CrossRef] [PubMed]
56. Yang, Y.P.; Giret, T.M.; Cote, R.J. Circulating Tumor Cells from Enumeration to Analysis: Current Challenges and Future Opportunities. *Cancers* **2021**, *13*, 2723. [CrossRef]
57. Andree, K.C.; van Dalum, G.; Terstappen, L.W. Challenges in circulating tumor cell detection by the CellSearch system. *Mol. Oncol.* **2016**, *10*, 395–407. [CrossRef]
58. Lemos, N.E.; Farias, M.G.; Kubaski, F.; Scotti, L.; Onsten, T.G.H.; Brondani, L.A.; Wagner, S.C.; Sekine, L. Quantification of peripheral blood CD34(+) cells prior to stem cell harvesting by leukapheresis: A single center experience. *Hematol. Transfus. Cell Ther.* **2018**, *40*, 213–218. [CrossRef]
59. Park, B.; Yoo, K.H.; Kim, C. Hematopoietic stem cell expansion and generation: The ways to make a breakthrough. *Blood Res.* **2015**, *50*, 194–203. [CrossRef]
60. Marquez-Curtis, L.A.; Turner, A.R.; Sridharan, S.; Ratajczak, M.Z.; Janowska-Wieczorek, A. The ins and outs of hematopoietic stem cells: Studies to improve transplantation outcomes. *Stem Cell Rev. Rep.* **2011**, *7*, 590–607. [CrossRef]
61. Rajendiran, S.; Boyer, S.W.; Forsberg, E.C. A quantitative hematopoietic stem cell reconstitution protocol: Accounting for recipient variability, tissue distribution and cell half-lives. *Stem Cell Res.* **2020**, *50*, 102145. [CrossRef]
62. Ben-David, U.; Gan, Q.F.; Golan-Lev, T.; Arora, P.; Yanuka, O.; Oren, Y.S.; Leikin-Frenkel, A.; Graf, M.; Garippa, R.; Boehringer, M.; et al. Selective elimination of human pluripotent stem cells by an oleate synthesis inhibitor discovered in a high-throughput screen. *Cell Stem Cell* **2013**, *12*, 167–179. [CrossRef]
63. Han, L.; He, H.; Yang, Y.; Meng, Q.; Ye, F.; Chen, G.; Zhang, J. Distinctive Clinical and Pathologic Features of Immature Teratomas Arising from Induced Pluripotent Stem Cell-Derived Beta Cell Injection in a Diabetes Patient. *Stem Cells Dev.* **2022**, *31*, 97–101. [CrossRef] [PubMed]
64. Hong, S.G.; Winkler, T.; Wu, C.; Guo, V.; Pittaluga, S.; Nicolae, A.; Donahue, R.E.; Metzger, M.E.; Price, S.D.; Uchida, N.; et al. Path to the clinic: Assessment of iPSC-based cell therapies in vivo in a nonhuman primate model. *Cell Rep.* **2014**, *7*, 1298–1309. [CrossRef] [PubMed]
65. Muller, F.J.; Goldmann, J.; Loser, P.; Loring, J.F. A call to standardize teratoma assays used to define human pluripotent cell lines. *Cell Stem Cell* **2010**, *6*, 412–414. [CrossRef] [PubMed]
66. Fong, C.Y.; Gauthaman, K.; Bongso, A. Teratomas from pluripotent stem cells: A clinical hurdle. *J. Cell Biochem.* **2010**, *111*, 769–781. [CrossRef] [PubMed]
67. Blum, B.; Benvenisty, N. The tumorigenicity of human embryonic stem cells. *Adv. Cancer Res.* **2008**, *100*, 133–158.
68. Lee, A.S.; Tang, C.; Rao, M.S.; Weissman, I.L.; Wu, J.C. Tumorigenicity as a clinical hurdle for pluripotent stem cell therapies. *Nat. Med.* **2013**, *19*, 998–1004. [CrossRef]
69. Wellmerling, K.; Lehmann, C.; Singh, A.; Kirby, B.J. Microfluidic chip for label-free removal of teratoma-forming cells from therapeutic human stem cells. *J. Immunol. Regen. Med.* **2020**, *10*, 100030. [CrossRef]
70. Chen, K.; Georgiev, T.Z.; Sheng, W.; Zheng, X.; Varillas, J.I.; Zhang, J.; Hugh Fan, Z. Tumor cell capture patterns around aptamer-immobilized microposts in microfluidic devices. *Biomicrofluidics* **2017**, *11*, 054110. [CrossRef]

71. Chen, K.; Dopico, P.; Varillas, J.; Zhang, J.; George, T.J.; Fan, Z.H. Integration of Lateral Filter Arrays with Immunoaffinity for Circulating-Tumor-Cell Isolation. *Angew. Chem. Int. Ed. Engl.* **2019**, *58*, 7606–7610. [CrossRef]
72. Green, B.J.; Marazzini, M.; Hershey, B.; Fardin, A.; Li, Q.; Wang, Z.; Giangreco, G.; Pisati, F.; Marchesi, S.; Disanza, A.; et al. PillarX: A Microfluidic Device to Profile Circulating Tumor Cell Clusters Based on Geometry, Deformability, and Epithelial State. *Small* **2022**, *18*, e2106097. [CrossRef]
73. Sarioglu, A.F.; Aceto, N.; Kojic, N.; Donaldson, M.C.; Zeinali, M.; Hamza, B.; Engstrom, A.; Zhu, H.; Sundaresan, T.K.; Miyamoto, D.T.; et al. A microfluidic device for label-free, physical capture of circulating tumor cell clusters. *Nat. Methods* **2015**, *12*, 685–691. [CrossRef] [PubMed]
74. Au, S.H.; Edd, J.; Stoddard, A.E.; Wong, K.H.K.; Fachin, F.; Maheswaran, S.; Haber, D.A.; Stott, S.L.; Kapur, R.; Toner, M. Microfluidic Isolation of Circulating Tumor Cell Clusters by Size and Asymmetry. *Sci. Rep.* **2017**, *7*, 2433. [CrossRef]
75. Varillas, J.I.; Zhang, J.; Chen, K.; Barnes, I.I.; Liu, C.; George, T.J.; Fan, Z.H. Microfluidic Isolation of Circulating Tumor Cells and Cancer Stem-Like Cells from Patients with Pancreatic Ductal Adenocarcinoma. *Theranostics* **2019**, *9*, 1417–1425. [CrossRef]
76. Cho, H.Y.; Choi, J.H.; Lim, J.; Lee, S.N.; Choi, J.W. Microfluidic Chip-Based Cancer Diagnosis and Prediction of Relapse by Detecting Circulating Tumor Cells and Circulating Cancer Stem Cells. *Cancers* **2021**, *13*, 1385. [CrossRef] [PubMed]
77. Obermayr, E.; Koppensteiner, N.; Heinzl, N.; Schuster, E.; Holzer, B.; Fabikan, H.; Weinlinger, C.; Illini, O.; Hochmair, M.; Zeillinger, R. Cancer Stem Cell-Like Circulating Tumor Cells Are Prognostic in Non-Small Cell Lung Cancer. *J. Pers. Med.* **2021**, *11*, 1225. [CrossRef]
78. Zhang, H.; Yang, Y.; Liu, Y.; Wang, Y.; Ruan, W.; Song, J.; Yu, X.; Wu, L.; Zhu, Z.; Hong, G.; et al. Stimuli-Responsive Microfluidic Interface Enables Highly Efficient Capture and Release of Circulating Fetal Cells for Non-Invasive Prenatal Testing. *Anal. Chem.* **2020**, *92*, 9281–9286. [CrossRef]
79. Winter, M.; Hardy, T.; Rezaei, M.; Nguyen, V.; Zander-Fox, D.; Ebrahimi Warkiani, M.; Thierry, B. Isolation of Circulating Fetal Trophoblasts Using Inertial Microfluidics for Noninvasive Prenatal Testing. *Adv. Mater. Technol.* **2018**, *3*, 1800066. [CrossRef]
80. Chen, S.; Sun, Y.; Neoh, K.H.; Chen, A.; Li, W.; Yang, X.; Han, R.P.S. Microfluidic assay of circulating endothelial cells in coronary artery disease patients with angina pectoris. *PLoS ONE* **2017**, *12*, e0181249. [CrossRef]
81. Wang, Z.; Sargent, E.H.; Kelley, S.O. Ultrasensitive Detection and Depletion of Rare Leukemic B Cells in T Cell Populations via Immunomagnetic Cell Ranking. *Anal. Chem.* **2021**, *93*, 2327–2335. [CrossRef]
82. Al-Khafaji, Q.A.M.; Harris, M.; Tombelli, S.; Laschi, S.; Turner, A.P.F.; Mascini, M.; Marrazza, G. An Electrochemical Immunoassay for HER2 Detection. *Electroanalysis* **2012**, *24*, 735–742. [CrossRef]
83. Liao, Z.Y.; Han, L.; Li, Q.J.; Li, L.Y.; Liu, Y.; Song, Y.; Tan, W.H.; Song, E.R. Gradient Magnetic Separation and Fluorescent Imaging-Based Heterogeneous Circulating Tumor Cell Subpopulations Assay with Biomimetic Multifunctional Nanoprobes. *Adv. Funct. Mater.* **2021**, *31*, 2009937. [CrossRef]
84. Chen, Y.; Wang, W.; Tyagi, D.; Carrier, A.J.; Cui, S.; He, S.; Zhang, X. Non-invasive isolation of rare circulating tumor cells with a DNA mimic of double-sided tape using multimeric aptamers. *Nanoscale* **2019**, *11*, 5879–5883. [CrossRef] [PubMed]
85. Berezovski, M.V.; Lechmann, M.; Musheev, M.U.; Mak, T.W.; Krylov, S.N. Aptamer-facilitated biomarker discovery (AptaBiD). *J. Am. Chem. Soc.* **2008**, *130*, 9137–9143. [CrossRef] [PubMed]
86. Kajani, A.A.; Rafiee, L.; Samandari, M.; Mehrgardi, M.A.; Zarrin, B.; Javanmard, S.H. Facile, rapid and efficient isolation of circulating tumor cells using aptamer-targeted magnetic nanoparticles integrated with a microfluidic device. *RSC Adv.* **2022**, *12*, 32834–32843. [CrossRef]
87. Liu, M.; Wang, J.; Chang, Y.; Zhang, Q.; Chang, D.; Hui, C.Y.; Brennan, J.D.; Li, Y. In Vitro Selection of a DNA Aptamer Targeting Degraded Protein Fragments for Biosensing. *Angew. Chem. Int. Ed. Engl.* **2020**, *59*, 7706–7710. [CrossRef]
88. Qian, S.; Chang, D.; He, S.; Li, Y. Aptamers from random sequence space: Accomplishments, gaps and future considerations. *Anal. Chim. Acta* **2022**, *1196*, 339511. [CrossRef] [PubMed]
89. Neumann, M.H.D.; Schneck, H.; Decker, Y.; Schomer, S.; Franken, A.; Endris, V.; Pfarr, N.; Weichert, W.; Niederacher, D.; Fehm, T.; et al. Isolation and characterization of circulating tumor cells using a novel workflow combining the CellSearch((R)) system and the CellCelector. *Biotechnol. Prog.* **2017**, *33*, 125–132. [CrossRef]
90. Wu, J.H.; Raba, K.; Guglielmi, R.; Behrens, B.; Van Dalum, G.; Flugen, G.; Koch, A.; Patel, S.; Knoefel, W.T.; Stoecklein, N.H.; et al. Magnetic-Based Enrichment of Rare Cells from High Concentrated Blood Samples. *Cancers* **2020**, *12*, 933. [CrossRef]
91. Shabatina, T.I.; Vernaya, O.I.; Shabatin, V.P.; Melnikov, M.Y. Magnetic Nanoparticles for Biomedical Purposes: Modern Trends and Prospects. *Magnetochemistry* **2020**, *6*, 30. [CrossRef]
92. Bohmer, N.; Demarmels, N.; Tsolaki, E.; Gerken, L.; Keevend, K.; Bertazzo, S.; Lattuada, M.; Herrmann, I.K. Removal of Cells from Body Fluids by Magnetic Separation in Batch and Continuous Mode: Influence of Bead Size, Concentration, and Contact Time. *ACS Appl. Mater. Interfaces* **2017**, *9*, 29571–29579. [CrossRef]
93. McDonald, J.U.; Ekeruche-Makinde, J.; Ho, M.M.; Tregoning, J.S.; Ashiru, O. Development of a custom pentaplex sandwich immunoassay using Protein-G coupled beads for the Luminex(R) xMAP(R) platform. *J. Immunol. Methods* **2016**, *433*, 6–16. [CrossRef] [PubMed]
94. Haukanes, B.I.; Kvam, C. Application of magnetic beads in bioassays. *Biotechnology* **1993**, *11*, 60–63. [CrossRef] [PubMed]
95. Castillo-Torres, K.Y.; McLamore, E.S.; Arnold, D.P. A High-throughput Microfluidic Magnetic Separation (mu FMS) Platform for Water Quality Monitoring. *Micromachines* **2020**, *11*, 16. [CrossRef]

96. Murray, C.; Pao, E.; Jann, A.; Park, D.E.; Di Carlo, D. Continuous and Quantitative Purification of T-Cell Subsets for Cell Therapy Manufacturing Using Magnetic Ratcheting Cytometry. *SLAS Technol.* **2018**, *23*, 326–337. [CrossRef] [PubMed]
97. Laghmouchi, A.; Hoogstraten, C.; Falkenburg, J.H.F.; Jedema, I. Long-term in vitro persistence of magnetic properties after magnetic bead-based cell separation of T cells. *Scand. J. Immunol.* **2020**, *92*, e12924. [CrossRef] [PubMed]
98. Berry, C.C.; Wells, S.; Charles, S.; Aitchison, G.; Curtis, A.S. Cell response to dextran-derivatised iron oxide nanoparticles post internalisation. *Biomaterials* **2004**, *25*, 5405–5413. [CrossRef] [PubMed]
99. Pisanic, T.R., 2nd; Blackwell, J.D.; Shubayev, V.I.; Finones, R.R.; Jin, S. Nanotoxicity of iron oxide nanoparticle internalization in growing neurons. *Biomaterials* **2007**, *28*, 2572–2581. [CrossRef]
100. Leigh, D.R.; Steinert, S.; Moore, L.R.; Chalmers, J.; Zborowski, M. Cell Tracking Velocimetry as a tool for defining saturation binding of magnetically conjugated antibodies. *Cytom. Part A* **2005**, *66*, 103–108. [CrossRef]
101. Zborowski, M.; Chalmers, J.J. Rare cell separation and analysis by magnetic sorting. *Anal. Chem.* **2011**, *83*, 8050–8056. [CrossRef]
102. Miltenyi, S.; Muller, W.; Weichel, W.; Radbruch, A. High gradient magnetic cell separation with MACS. *Cytometry* **1990**, *11*, 231–238. [CrossRef]
103. Sleijfer, S.; Gratama, J.-W.; Sieuwerts, A.M.; Kraan, J.; Martens, J.W.; Foekens, J.A. Circulating tumour cell detection on its way to routine diagnostic implementation? *Eur. J. Cancer* **2007**, *43*, 2645–2650. [CrossRef] [PubMed]
104. Tewes, M.; Aktas, B.; Welt, A.; Mueller, S.; Hauch, S.; Kimmig, R.; Kasimir-Bauer, S. Molecular profiling and predictive value of circulating tumor cells in patients with metastatic breast cancer: An option for monitoring response to breast cancer related therapies. *Breast Cancer Res. Treat.* **2009**, *115*, 581–590. [CrossRef]
105. Royet, D.; Heriveaux, Y.; Marchalot, J.; Scorretti, R.; Dias, A.; Dempsey, N.M.; Bonfim, M.; Simonet, P.; Frenea-Robin, M. Using injection molding and reversible bonding for easy fabrication of magnetic cell trapping and sorting devices. *J. Magn. Magn. Mater.* **2017**, *427*, 306–313. [CrossRef]
106. Mair, B.; Aldridge, P.M.; Atwal, R.S.; Philpott, D.; Zhang, M.; Masud, S.N.; Labib, M.; Tong, A.H.Y.; Sargent, E.H.; Angers, S.; et al. High-throughput genome-wide phenotypic screening via immunomagnetic cell sorting. *Nat. Biomed. Eng.* **2019**, *3*, 796–805. [CrossRef]
107. Zhao, W.; Cheng, R.; Lim, S.H.; Miller, J.R.; Zhang, W.; Tang, W.; Xie, J.; Mao, L. Biocompatible and label-free separation of cancer cells from cell culture lines from white blood cells in ferrofluids. *Lab Chip* **2017**, *17*, 2243–2255. [CrossRef] [PubMed]
108. Kang, J.H.; Krause, S.; Tobin, H.; Mammoto, A.; Kanapathipillai, M.; Ingber, D.E. A combined micromagnetic-microfluidic device for rapid capture and culture of rare circulating tumor cells. *Lab Chip* **2012**, *12*, 2175–2181. [CrossRef]
109. Zhao, W.; Zhu, T.; Cheng, R.; Liu, Y.; He, J.; Qiu, H.; Wang, L.; Nagy, T.; Querec, T.D.; Unger, E.R.; et al. Label-Free and Continuous-Flow Ferrohydrodynamic Separation of HeLa Cells and Blood Cells in Biocompatible Ferrofluids. *Adv. Funct. Mater.* **2016**, *26*, 3990–3998. [CrossRef] [PubMed]
110. Unni, M.; Zhang, J.L.; George, T.J.; Segal, M.S.; Fan, Z.H.; Rinaldi, C. Engineering magnetic nanoparticles and their integration with microfluidics for cell isolation. *J. Colloid Interface Sci.* **2020**, *564*, 204–215. [CrossRef]
111. Hoshino, K.; Huang, Y.-Y.; Lane, N.; Huebschman, M.; Uhr, J.W.; Frenkel, E.P.; Zhang, X. Microchip-based immunomagnetic detection of circulating tumor cells. *Lab Chip* **2011**, *11*, 3449–3457. [CrossRef]
112. Labib, M.; Wang, Z.; Ahmed, S.U.; Mohamadi, R.M.; Duong, B.; Green, B.; Sargent, E.H.; Kelley, S.O. Tracking the expression of therapeutic protein targets in rare cells by antibody-mediated nanoparticle labelling and magnetic sorting. *Nat. Biomed. Eng.* **2021**, *5*, 41–52. [CrossRef]
113. Khojah, R.; Xiao, Z.; Panduranga, M.K.; Bogumil, M.; Wang, Y.; Goiriena-Goikoetxea, M.; Chopdekar, R.V.; Bokor, J.; Carman, G.P.; Candler, R.N.; et al. Single-Domain Multiferroic Array-Addressable Terfenol-D (SMArT) Micromagnets for Programmable Single-Cell Capture and Release. *Adv. Mater.* **2021**, *33*, e2006651. [CrossRef] [PubMed]
114. Lin, S.; Zhi, X.; Chen, D.; Xia, F.; Shen, Y.; Niu, J.; Huang, S.; Song, J.; Miao, J.; Cui, D.; et al. A flyover style microfluidic chip for highly purified magnetic cell separation. *Biosens. Bioelectron.* **2019**, *129*, 175–181. [CrossRef] [PubMed]
115. Yu, X.; Feng, X.; Hu, J.; Zhang, Z.L.; Pang, D.W. Controlling the magnetic field distribution on the micrometer scale and generation of magnetic bead patterns for microfluidic applications. *Langmuir ACS J. Surf. Colloids* **2011**, *27*, 5147–5156. [CrossRef]
116. Inglis, D.W.; Riehn, R.; Austin, R.H.; Sturm, J.C. Continuous microfluidic immunomagnetic cell separation. *Appl. Phys. Lett.* **2004**, *85*, 5093–5095. [CrossRef]
117. Lou, X.; Qian, J.; Xiao, Y.; Viel, L.; Gerdon, A.E.; Lagally, E.T.; Atzberger, P.; Tarasow, T.M.; Heeger, A.J.; Soh, H.T. Micromagnetic selection of aptamers in microfluidic channels. *Proc. Natl. Acad. Sci. USA* **2009**, *106*, 2989–2994. [CrossRef] [PubMed]
118. Murray, C.; Miwa, H.; Dhar, M.; Park, D.E.; Pao, E.; Martinez, J.; Kaanumale, S.; Loghin, E.; Graf, J.; Rhaddassi, K. Unsupervised capture and profiling of rare immune cells using multi-directional magnetic ratcheting. *Lab Chip* **2018**, *18*, 2396–2409. [CrossRef]
119. Adeyiga, O.B.; Murray, C.; Muñoz, H.E.; Escobar, A.; Di Carlo, D. Magnetic microparticle concentration and collection using a mechatronic magnetic ratcheting system. *PLoS ONE* **2021**, *16*, e0246124. [CrossRef]
120. Aldridge, P.M.; Mukhopadhyay, M.; Ahmed, S.U.; Zhou, W.; Christinck, E.; Makonnen, R.; Sargent, E.H.; Kelley, S.O. Prismatic Deflection of Live Tumor Cells and Cell Clusters. *ACS Nano* **2018**, *12*, 12692–12700. [CrossRef]
121. Philpott, D.N.; Chen, K.; Atwal, R.S.; Li, D.; Christie, J.; Sargent, E.H.; Kelley, S.O. Ultrathroughput immunomagnetic cell sorting platform. *Lab Chip* **2022**, *22*, 4822–4830. [CrossRef]
122. Ma, Y.; Chen, K.; Xia, F.; Atwal, R.; Wang, H.; Ahmed, S.U.; Cardarelli, L.; Lui, I.; Duong, B.; Wang, Z.; et al. Phage-Based Profiling of Rare Single Cells Using Nanoparticle-Directed Capture. *ACS Nano* **2021**, *15*, 19202–19210. [CrossRef]

123. Fernandez, C.G.; Pastora, J.G.; Basauri, A.; Fallanza, M.; Bringas, E.; Chalmers, J.J.; Ortiz, I. Continuous-Flow Separation of Magnetic Particles from Biofluids: How Does the Microdevice Geometry Determine the Separation Performance? *Sensors* **2020**, *20*, 3030. [CrossRef] [PubMed]
124. Huang, N.T.; Hwong, Y.J.; Lai, R.L. A microfluidic microwell device for immunomagnetic single-cell trapping. *Microfluid. Nanofluid.* **2018**, *22*, 16. [CrossRef]
125. Shi, W.; Wang, S.; Maarouf, A.; Uhl, C.G.; He, R.; Yunus, D.; Liu, Y. Magnetic particles assisted capture and release of rare circulating tumor cells using wavy-herringbone structured microfluidic devices. *Lab Chip* **2017**, *17*, 3291–3299. [CrossRef] [PubMed]
126. Shen, Y.; Yalikun, Y.; Tanaka, Y. Recent advances in microfluidic cell sorting systems. *Sens. Actuators B Chem.* **2019**, *282*, 268–281. [CrossRef]
127. Yu, Z.T.F.; Aw Yong, K.M.; Fu, J. Microfluidic Blood Cell Sorting: Now and Beyond. *Small* **2014**, *10*, 1687–1703. [CrossRef] [PubMed]
128. Yun, H.; Kim, K.; Lee, W.G. Cell manipulation in microfluidics. *Biofabrication* **2013**, *5*, 022001. [CrossRef] [PubMed]
129. Marrinucci, D.; Bethel, K.; Kolatkar, A.; Luttgen, M.S.; Malchiodi, M.; Baehring, F.; Voigt, K.; Lazar, D.; Nieva, J.; Bazhenova, L.; et al. Fluid biopsy in patients with metastatic prostate, pancreatic and breast cancers. *Phys. Biol.* **2012**, *9*, 016003. [CrossRef]
130. Lang, J.M.; Casavant, B.P.; Beebe, D.J. Circulating Tumor Cells: Getting More from Less. *Sci. Transl. Med.* **2012**, *4*, 141ps13. [CrossRef]
131. Hyun, K.A.; Koo, G.B.; Han, H.; Sohn, J.; Choi, W.; Kim, S.I.; Jung, H.I.; Kim, Y.S. Epithelial-to-mesenchymal transition leads to loss of EpCAM and different physical properties in circulating tumor cells from metastatic breast cancer. *Oncotarget* **2016**, *7*, 24677–24687. [CrossRef]
132. Sankpal, N.V.; Fleming, T.P.; Sharma, P.K.; Wiedner, H.J.; Gillanders, W.E. A double-negative feedback loop between EpCAM and ERK contributes to the regulation of epithelial–mesenchymal transition in cancer. *Oncogene* **2017**, *36*, 3706–3717. [CrossRef]
133. Keller, L.; Werner, S.; Pantel, K. Biology and clinical relevance of EpCAM. *Cell Stress* **2019**, *3*, 165–180. [CrossRef] [PubMed]
134. Tellez-Gabriel, M.; Heymann, M.-F.; Heymann, D. Circulating Tumor Cells as a Tool for Assessing Tumor Heterogeneity. *Theranostics* **2019**, *9*, 4580–4594. [CrossRef]
135. Issadore, D.; Chung, J.; Shao, H.; Liong, M.; Ghazani, A.A.; Castro, C.M.; Weissleder, R.; Lee, H. Ultrasensitive Clinical Enumeration of Rare Cells ex vivo Using a Micro-Hall Detector. *Sci. Transl. Med.* **2012**, *4*, 141ra92. [CrossRef]
136. Scharpenseel, H.; Hanssen, A.; Loges, S.; Mohme, M.; Bernreuther, C.; Peine, S.; Lamszus, K.; Goy, Y.; Petersen, C.; Westphal, M.; et al. EGFR and HER3 expression in circulating tumor cells and tumor tissue from non-small cell lung cancer patients. *Sci. Rep.* **2019**, *9*, 7406. [CrossRef]
137. Broersen, L.H.A.; van Pelt, G.W.; Tollenaar, R.A.E.M.; Mesker, W.E. Clinical application of circulating tumor cells in breast cancer. *Cell. Oncol.* **2014**, *37*, 9–15. [CrossRef] [PubMed]
138. Menyailo, M.E.; Tretyakova, M.S.; Denisov, E.V. Heterogeneity of Circulating Tumor Cells in Breast Cancer: Identifying Metastatic Seeds. *Int. J. Mol. Sci.* **2020**, *21*, 1696. [CrossRef] [PubMed]
139. Jie, X.-X.; Zhang, X.-Y.; Xu, C.-J. Epithelial-to-mesenchymal transition, circulating tumor cells and cancer metastasis: Mechanisms and clinical applications. *Oncotarget* **2017**, *8*, 81558. [CrossRef]
140. Yin, D.; Shi, A.; Zhou, B.; Wang, M.; Xu, G.; Shen, M.; Zhu, X.; Shi, X. Efficient Capture and Separation of Cancer Cells Using Hyaluronic Acid-Modified Magnetic Beads in a Microfluidic Chip. *Langmuir ACS J. Surf. Colloids* **2022**, *38*, 11080–11086. [CrossRef] [PubMed]
141. Qin, D.; Xia, Y.; Whitesides, G.M. Soft lithography for micro- and nanoscale patterning. *Nat. Protoc.* **2010**, *5*, 491–502. [CrossRef]
142. Adams, J.D.; Kim, U.; Soh, H.T. Multitarget magnetic activated cell sorter. *Proc. Natl. Acad. Sci. USA* **2008**, *105*, 18165–18170. [CrossRef]
143. Nasiri, R.; Shamloo, A.; Akbari, J. Design of a Hybrid Inertial and Magnetophoretic Microfluidic Device for CTCs Separation from Blood. *Micromachines* **2021**, *12*, 877. [CrossRef] [PubMed]
144. Cetin, B.; Ozer, M.B.; Cagatay, E.; Buyukkocak, S. An integrated acoustic and dielectrophoretic particle manipulation in a microfluidic device for particle wash and separation fabricated by mechanical machining. *Biomicrofluidics* **2016**, *10*, 014112. [CrossRef]
145. Krishnan, J.N.; Kim, C.; Park, H.J.; Kang, J.Y.; Kim, T.S.; Kim, S.K. Rapid microfluidic separation of magnetic beads through dielectrophoresis and magnetophoresis. *Electrophoresis* **2009**, *30*, 1457–1463. [CrossRef] [PubMed]
146. Kim, U.; Soh, H.T. Simultaneous sorting of multiple bacterial targets using integrated Dielectrophoretic-Magnetic Activated Cell Sorter. *Lab Chip* **2009**, *9*, 2313–2318. [CrossRef]
147. Adams, J.D.; Thevoz, P.; Bruus, H.; Soh, H.T. Integrated acoustic and magnetic separation in microfluidic channels. *Appl. Phys. Lett.* **2009**, *95*, 254103. [CrossRef] [PubMed]
148. Alipanah, M.; Hafttananian, M.; Hedayati, N.; Ramiar, A.; Alipanah, M. Microfluidic on-demand particle separation using induced charged electroosmotic flow and magnetic field. *J. Magn. Magn. Mater.* **2021**, *537*, 168156. [CrossRef]
149. Shamloo, A.; Naghdloo, A.; Besanjideh, M. Cancer cell enrichment on a centrifugal microfluidic platform using hydrodynamic and magnetophoretic techniques. *Sci. Rep.* **2021**, *11*, 1939. [CrossRef]

150. Lin, Z.; Lin, S.-Y.; Xie, P.; Lin, C.-Y.; Rather, G.M.; Bertino, J.R.; Javanmard, M. Rapid assessment of surface markers on cancer cells using immuno-magnetic separation and multi-frequency impedance cytometry for targeted therapy. *Sci. Rep.* **2020**, *10*, 3015. [CrossRef]
151. Mishra, A.; Dubash, T.D.; Edd, J.F.; Jewett, M.K.; Garre, S.G.; Karabacak, N.M.; Rabe, D.C.; Mutlu, B.R.; Walsh, J.R.; Kapur, R.; et al. Ultrahigh-throughput magnetic sorting of large blood volumes for epitope-agnostic isolation of circulating tumor cells. *Proc. Natl. Acad. Sci. USA* **2020**, *117*, 16839–16847. [CrossRef]
152. Yoo, C.E.; Park, J.-M.; Moon, H.-S.; Joung, J.-G.; Son, D.-S.; Jeon, H.-J.; Kim, Y.J.; Han, K.-Y.; Sun, J.-M.; Park, K.; et al. Vertical Magnetic Separation of Circulating Tumor Cells for Somatic Genomic-Alteration Analysis in Lung Cancer Patients. *Sci. Rep.* **2016**, *6*, 37392. [CrossRef]
153. Yu, T.; Wang, C.; Xie, M.; Zhu, C.; Shu, Y.; Tang, J.; Guan, X. Heterogeneity of CTC contributes to the organotropism of breast cancer. *Biomed. Pharmacother.* **2021**, *137*, 111314. [CrossRef] [PubMed]
154. Saxena, K.; Subbalakshmi, A.R.; Jolly, M.K. Phenotypic heterogeneity in circulating tumor cells and its prognostic value in metastasis and overall survival. *eBioMedicine* **2019**, *46*, 4–5. [CrossRef] [PubMed]
155. Mohamadi, R.M.; Besant, J.D.; Mepham, A.; Green, B.; Mahmoudian, L.; Gibbs, T.; Ivanov, I.; Malvea, A.; Stojcic, J.; Allan, A.L.; et al. Nanoparticle-mediated binning and profiling of heterogeneous circulating tumor cell subpopulations. *Angew. Chem. Int. Ed. Engl.* **2015**, *54*, 139–143. [CrossRef] [PubMed]
156. Poudineh, M.; Aldridge, P.M.; Ahmed, S.; Green, B.J.; Kermanshah, L.; Nguyen, V.; Tu, C.; Mohamadi, R.M.; Nam, R.K.; Hansen, A.; et al. Tracking the dynamics of circulating tumour cell phenotypes using nanoparticle-mediated magnetic ranking. *Nat. Nanotechnol.* **2017**, *12*, 274–281. [CrossRef]
157. Leggett, S.E.; Wong, I.Y. Nanomedicine: Catching tumour cells in the zone. *Nat. Nanotechnol.* **2017**, *12*, 191–193. [CrossRef]
158. Bass, R.; Roberto, D.; Wang, D.Z.; Cantu, F.P.; Mohamadi, R.M.; Kelley, S.O.; Klotz, L.; Venkateswaran, V. Combining Desmopressin and Docetaxel for the Treatment of Castration-Resistant Prostate Cancer in an Orthotopic Model. *Anticancer Res.* **2019**, *39*, 113–118. [CrossRef]
159. Green, B.J.; Kermanshah, L.; Labib, M.; Ahmed, S.U.; Silva, P.N.; Mahmoudian, L.; Chang, I.H.; Mohamadi, R.M.; Rocheleau, J.V.; Kelley, S.O. Isolation of Phenotypically Distinct Cancer Cells Using Nanoparticle-Mediated Sorting. *ACS Appl. Mater. Interfaces* **2017**, *9*, 20435–20443. [CrossRef]
160. Labib, M.; Philpott, D.N.; Wang, Z.; Nemr, C.; Chen, J.B.; Sargent, E.H.; Kelley, S.O. Magnetic Ranking Cytometry: Profiling Rare Cells at the Single-Cell Level. *ACC Chem. Res.* **2020**, *53*, 1445–1457. [CrossRef]
161. Zongjie, W.; Mark, G.; Reza, M.; Sharif, A.; Mahmoud, L.; Libing, Z.; Sandra, P.; Yuxiao, Z.; Edward, S.; Gordon, K.; et al. Ultrasensitive and rapid quantification of rare tumorigenic stem cells in hPSC-derived cardiomyocyte populations. *Sci. Adv.* **2020**, *6*, eaay7629.
162. Duong, B.T.V.; Wu, L.; Green, B.J.; Bavaghar-Zaeimi, F.; Wang, Z.; Labib, M.; Zhou, Y.; Cantu, F.J.P.; Jeganathan, T.; Popescu, S.; et al. A liquid biopsy for detecting circulating mesothelial precursor cells: A new biomarker for diagnosis and prognosis in mesothelioma. *eBioMedicine* **2020**, *61*, 103031. [CrossRef]
163. Poudineh, M.; Labib, M.; Ahmed, S.; Nguyen, L.N.; Kermanshah, L.; Mohamadi, R.M.; Sargent, E.H.; Kelley, S.O. Profiling Functional and Biochemical Phenotypes of Circulating Tumor Cells Using a Two-Dimensional Sorting Device. *Angew. Chem. Int. Ed. Engl.* **2017**, *56*, 163–168. [CrossRef] [PubMed]
164. Knoepfler, P.S. Deconstructing stem cell tumorigenicity: A roadmap to safe regenerative medicine. *Stem Cells* **2009**, *27*, 1050–1056. [CrossRef] [PubMed]
165. Ben-David, U.; Benvenisty, N. The tumorigenicity of human embryonic and induced pluripotent stem cells. *Nat. Rev. Cancer* **2011**, *11*, 268–277. [CrossRef] [PubMed]
166. Hentze, H.; Soong, P.L.; Wang, S.T.; Phillips, B.W.; Putti, T.C.; Dunn, N.R. Teratoma formation by human embryonic stem cells: Evaluation of essential parameters for future safety studies. *Stem Cell Res.* **2009**, *2*, 198–210. [CrossRef]
167. Wang, Z.; Ahmed, S.; Labib, M.; Wang, H.; Wu, L.; Bavaghar-Zaeimi, F.; Shokri, N.; Blanco, S.; Karim, S.; Czarnecka-Kujawa, K.; et al. Isolation of tumour-reactive lymphocytes from peripheral blood via microfluidic immunomagnetic cell sorting. *Nat. Biomed. Eng*. 2023. *Online ahead of print*. Available online: https://www.nature.com/articles/s41551-023-01023-3 (accessed on 21 May 2023).
168. Yoseph, R.; Krishna, S.; Lowery, F.J.; Copeland, A.R.; Parikh, N.B.; Hitscherich, K.; Robbins, P.F.; Rosenberg, S.A. Single-cell analysis of circulating neoantigen-reactive $CD8^+$ T cells allows isolation of novel tumor reactive TCRs. *Cancer Res.* **2022**, *82*, 2762. [CrossRef]
169. Chang, D.; Zongjie, W.; Flynn, C.; Mahmud, A.; Labib, M.; Wang, H.; Geraili, A.; Li, X.; Zhang, J.; Sargent, E.; et al. A high-dimensional microfluidic approach for selection of aptamers with programmable binding affinities. *Nat. Chem.* **2023**, *15*, 773–780. [CrossRef]
170. Noosawat, P.; Srituravanich, W.; Damrongplasit, N.; Suzuki, Y.; Kaewthamasorn, M.; Pimpin, A. A microfluidic device for capturing malaria-infected red blood cells by magnetophoretic force using an array of V- and W-shaped nickel microstructures. *Microfluid. Nanofluid.* **2022**, *26*, 78. [CrossRef]
171. Descamps, L.; Garcia, J.; Barthelemy, D.; Laurenceau, E.; Payen, L.; Le Roy, D.; Deman, A.L. MagPure chip: An immunomagnetic-based microfluidic device for high purification of circulating tumor cells from liquid biopsies. *Lab Chip* **2022**, *22*, 4151–4166. [CrossRef]

172. Lim, S.B.; Lim, C.T.; Lim, W.T. Single-Cell Analysis of Circulating Tumor Cells: Why Heterogeneity Matters. *Cancers* **2019**, *11*, 1595. [CrossRef]
173. Keller, L.; Pantel, K. Unravelling tumour heterogeneity by single-cell profiling of circulating tumour cells. *Nat. Rev. Cancer* **2019**, *19*, 553–567. [CrossRef]
174. Romero, D. Breast cancer: CTC heterogeneity is dynamic. *Nat. Rev. Clin. Oncol.* **2016**, *13*, 654. [CrossRef] [PubMed]
175. Mego, M.; De Giorgi, U.; Dawood, S.; Wang, X.; Valero, V.; Andreopoulou, E.; Handy, B.; Ueno, N.T.; Reuben, J.M.; Cristofanilli, M. Characterization of metastatic breast cancer patients with nondetectable circulating tumor cells. *Int. J. Cancer* **2011**, *129*, 417–423. [CrossRef] [PubMed]
176. de Wit, S.; van Dalum, G.; Lenferink, A.T.; Tibbe, A.G.; Hiltermann, T.J.; Groen, H.J.; van Rijn, C.J.; Terstappen, L.W. The detection of EpCAM(+) and EpCAM(−) circulating tumor cells. *Sci. Rep.* **2015**, *5*, 12270. [CrossRef] [PubMed]
177. Gazzaniga, P.; Raimondi, C.; Gradilone, A.; Di Seri, M.; Longo, F.; Cortesi, E.; Frati, L. Circulating tumor cells, colon cancer and bevacizumab: The meaning of zero. *Ann. Oncol.* **2011**, *22*, 1929–1930. [CrossRef]
178. Lin, D.; Shen, L.; Luo, M.; Zhang, K.; Li, J.; Yang, Q.; Zhu, F.; Zhou, D.; Zheng, S.; Chen, Y.; et al. Circulating tumor cells: Biology and clinical significance. *Signal Transduct. Target. Ther.* **2021**, *6*, 404. [CrossRef]
179. Wang, Y.; Liu, Y.; Zhang, L.; Tong, L.; Gao, Y.; Hu, F.; Lin, P.P.; Li, B.; Zhang, T. Vimentin expression in circulating tumor cells (CTCs) associated with liver metastases predicts poor progression-free survival in patients with advanced lung cancer. *J. Cancer Res. Clin. Oncol.* **2019**, *145*, 2911–2920. [CrossRef]
180. Po, J.W.; Roohullah, A.; Lynch, D.; DeFazio, A.; Harrison, M.; Harnett, P.R.; Kennedy, C.; de Souza, P.; Becker, T.M. Improved ovarian cancer EMT-CTC isolation by immunomagnetic targeting of epithelial EpCAM and mesenchymal N-cadherin. *J. Circ. Biomark.* **2018**, *7*, 1849454418782617. [CrossRef]
181. Bastos, D.A.; Antonarakis, E.S. CTC-derived AR-V7 detection as a prognostic and predictive biomarker in advanced prostate cancer. *Expert. Rev. Mol. Diagn.* **2018**, *18*, 155–163. [CrossRef]
182. Riethdorf, S.; Muller, V.; Zhang, L.; Rau, T.; Loibl, S.; Komor, M.; Roller, M.; Huober, J.; Fehm, T.; Schrader, I.; et al. Detection and HER2 expression of circulating tumor cells: Prospective monitoring in breast cancer patients treated in the neoadjuvant GeparQuattro trial. *Clin. Cancer Res.* **2010**, *16*, 2634–2645. [CrossRef]
183. Lindsay, C.R.; Le Moulec, S.; Billiot, F.; Loriot, Y.; Ngo-Camus, M.; Vielh, P.; Fizazi, K.; Massard, C.; Farace, F. Vimentin and Ki67 expression in circulating tumour cells derived from castrate-resistant prostate cancer. *BMC Cancer* **2016**, *16*, 168. [CrossRef]
184. Wang, Z.; Xia, F.; Labib, M.; Ahmadi, M.; Chen, H.; Das, J.; Ahmed, S.U.; Angers, S.; Sargent, E.H.; Kelley, S.O. Nanostructured Architectures Promote the Mesenchymal-Epithelial Transition for Invasive Cells. *ACS Nano* **2020**, *14*, 5324–5336. [CrossRef]
185. Cao, T.; Rajasingh, S.; Rajasingh, J. Circulating fibrocytes serve as a marker for clinical diagnosis. *Ann. Transl. Med.* **2016**, *4* (Suppl. S1), S38. [CrossRef] [PubMed]
186. Labib, M.; Green, B.; Mohamadi, R.M.; Mepham, A.; Ahmed, S.U.; Mahmoudian, L.; Chang, I.H.; Sargent, E.H.; Kelley, S.O. Aptamer and Antisense-Mediated Two-Dimensional Isolation of Specific Cancer Cell Subpopulations. *J. Am. Chem. Soc.* **2016**, *138*, 2476–2479. [CrossRef] [PubMed]
187. Cheng, O.H.-C.; Son, D.H.; Sheldon, M. Light-induced magnetism in plasmonic gold nanoparticles. *Nat. Photonics* **2020**, *14*, 365–368. [CrossRef]
188. Liu, Y.; Lin, G.; Chen, Y.; Monch, I.; Makarov, D.; Walsh, B.J.; Jin, D. Coding and decoding stray magnetic fields for multiplexing kinetic bioassay platform. *Lab Chip* **2020**, *20*, 4561–4571. [CrossRef] [PubMed]
189. Wang, Z.; Samanipour, R.; Gamaleldin, M.; Sakthivel, K.; Kim, K. An automated system for high-throughput generation and optimization of microdroplets. *Biomicrofluidics* **2016**, *10*, 054110. [CrossRef]
190. Wang, Z.; Tian, Z.; Menard, F.; Kim, K. Comparative study of gelatin methacrylate hydrogels from different sources for biofabrication applications. *Biofabrication* **2017**, *9*, 044101. [CrossRef]
191. de Rutte, J.; Dimatteo, R.; Archang, M.M.; van Zee, M.; Koo, D.; Lee, S.; Sharrow, A.C.; Krohl, P.J.; Mellody, M.; Zhu, S.; et al. Suspendable Hydrogel Nanovials for Massively Parallel Single-Cell Functional Analysis and Sorting. *ACS Nano* **2022**, *16*, 7242–7257. [CrossRef]
192. Miwa, H.; Dimatteo, R.; de Rutte, J.; Ghosh, R.; Di Carlo, D. Single-cell sorting based on secreted products for functionally defined cell therapies. *Microsyst. Nanoeng.* **2022**, *8*, 84. [CrossRef]
193. Mohamed, M.; Kumar, H.; Wang, Z.; Martin, N.; Mills, B.; Kim, K. Rapid and Inexpensive Fabrication of Multi-Depth Microfluidic Device using High-Resolution LCD Stereolithographic 3D Printing. *J. Manuf. Mater. Process.* **2019**, *3*, 26. [CrossRef]
194. Wang, Z.; Martin, N.; Hini, D.; Mills, B.; Kim, K. Rapid Fabrication of Multilayer Microfluidic Devices Using the Liquid Crystal Display-Based Stereolithography 3D Printing System. *3D Print. Addit. Manuf.* **2017**, *4*, 156–164. [CrossRef]
195. Ahmed, I.; Sullivan, K.; Priye, A. Multi-Resin Masked Stereolithography (MSLA) 3D Printing for Rapid and Inexpensive Prototyping of Microfluidic Chips with Integrated Functional Components. *Biosensors* **2022**, *12*, 652. [CrossRef]
196. Ibi, T.; Komada, E.; Furukawa, T.; Maruo, S. Multi-scale, multi-depth lithography using optical fibers for microfluidic applications. *Microfluid. Nanofluid.* **2018**, *22*, 69. [CrossRef]
197. Kjar, A.; Huang, Y. Application of Micro-Scale 3D Printing in Pharmaceutics. *Pharmaceutics* **2019**, *11*, 390. [CrossRef]
198. Behroodi, E.; Latifi, H.; Bagheri, Z.; Ermis, E.; Roshani, S.; Salehi Moghaddam, M. A combined 3D printing/CNC micro-milling method to fabricate a large-scale microfluidic device with the small size 3D architectures: An application for tumor spheroid production. *Sci. Rep.* **2020**, *10*, 22171. [CrossRef] [PubMed]

199. Gyimah, N.; Scheler, O.; Rang, T.; Pardy, T. Can 3D Printing Bring Droplet Microfluidics to Every Lab?—A Systematic Review. *Micromachines* **2021**, *12*, 339. [CrossRef] [PubMed]
200. Lin, H.; Yu, W.; Sabet, K.A.; Bogumil, M.; Zhao, Y.; Hambalek, J.; Lin, S.; Chandrasekaran, S.; Garner, O.; Di Carlo, D.; et al. Ferrobotic swarms enable accessible and adaptable automated viral testing. *Nature* **2022**, *611*, 570–577. [CrossRef]
201. Kim, S.-H.; Kim, K.; Go, M.; Park, J.Y. Stand-alone external power-free microfluidic fuel cell system harnessing osmotic pump for long-term operation. *J. Micromech. Microeng.* **2018**, *28*, 125005. [CrossRef]
202. Hosokawa, K. Biomarker Analysis on a Power-free Microfluidic Chip Driven by Degassed Poly(dimethylsiloxane). *Anal. Sci.* **2021**, *37*, 399–406. [CrossRef]
203. Wang, Z.; Boddeda, A.; Parker, B.; Samanipour, R.; Ghosh, S.; Menard, F.; Kim, K. A High-Resolution Minimicroscope System for Wireless Real-Time Monitoring. *IEEE Trans. Biomed. Eng.* **2018**, *65*, 1524–1531. [CrossRef]
204. Zhang, Y.S.; Ribas, J.; Nadhman, A.; Aleman, J.; Selimovic, S.; Lesher-Perez, S.C.; Wang, T.; Manoharan, V.; Shin, S.R.; Damilano, A.; et al. A cost-effective fluorescence mini-microscope for biomedical applications. *Lab Chip* **2015**, *15*, 3661–3669. [CrossRef] [PubMed]
205. Kim, S.B.; Koo, K.I.; Bae, H.; Dokmeci, M.R.; Hamilton, G.A.; Bahinski, A.; Kim, S.M.; Ingber, D.E.; Khademhosseini, A. A mini-microscope for in situ monitoring of cells. *Lab Chip* **2012**, *12*, 3976–3982. [CrossRef] [PubMed]